The family's physical burden increased significantly after the intervention of the SHPC service. The family experienced negative health changes, as has been suggested by previous studies.[19] Caring for a patient with terminal illness at home involves a considerable commitment on the part of family caregivers.[20] However, there has been a dearth of intervention studies undertaken to address unmet problems facing family caregivers of terminal cancer patients.[21] However, it is note worthy that anxiety regarding care at home, as measured in this study, was significantly mitigated. By receiving the SHPC service, it is likely that families benefited from an increased peace of mind regarding care at home, although families expressed physical burden. This result suggests one of the major positive impacts of the SHPC service. Psychosocial care for family during the palliative care phase has been emphasized in previous studies[22,23] as important care for continuing to provide care at home.

This study has several limitations. First, data was not obtained from all patients. The results may not generalize to all terminal cancer patients and their family at home. The largest cause of missing data in the study resulted from a patient's functional deterioration or death. Second, this study was limited to symptoms, a simple health-related quality-of-life scale, and ad hoc family variables. In-depth insights of the patients and their families should be included in future studies. Also, how to approach the time when sufficient verbal communication with a patient becomes difficult is our future task. Third, we did not compare our results with other settings. To develop SHPC service, it will be necessary to establish clinically suitable evaluation process of palliative care at home, and to examine carefully feasibility of the SHPC service in other areas of Japan.

Conclusion

Regarding patient characteristics at the time of referral to the SHPC service, patients referred from outpatient settings had more severe physical symptoms than patients referred from inpatient settings. The SHPC service could contribute to patients' symptoms and families' psychosocial status. On the whole, the evaluation of the SHPC service was positive during the 2-week period after starting home care.

Acknowledgments

We wish to thank the patients and their families who agreed to take part in the study. We are thankful to each and every one of all the staff of Okabe Clinic for their help.

References

1. Bruera E, Sweeney C. Palliative care models: international perspective. *J Palliat Med.* 2002;5:319-317.
2. Ida E, Miyachi M, Uemura M, Osakama M, Tajitsu T. Current status of hospice cancer deaths both in-unit and at home (1995-2000), and prospects of home care services in Japan. *Palliat Med.* 2002;16:179-184.
3. Fukui S, Kawagoe H, Masako S, Noriko N, Hiroko N, Toshie M. Determinants of the place of death among terminally ill cancer patients under home hospice care in Japan. *Palliat Med.* 2003;17:445-453.
4. Minister's Secretariat, Ministry of Health, Labor and Welfare. Vital Statistics (online). 2006; Available at http:// www.dbtk.mhlw.go.jp/toukei/data/010/2006/toukeihyou/ 0006067/t0134568/MC210000_001.html. Accessed January 13, 2009 (in Japanese).
5. Minister's Secretariat, Ministry of Health, Labor and Welfare. Report on Opinion Survey Regarding End of Life Care (online). 2004; Available at http://www.mhlw.go.jp/shingi/2004/2007/s0723-2008.html. Accessed January 13, 2009 (in Japanese).
6. Finlay IG, Higginson IJ, Goodwin DM, et al. Palliative care in hospital, hospice, at home: results from a systematic review. *Ann Oncol.* 2002;13(suppl 4):257-264.
7. Ronaldson S, Devery K. The experience of transition to palliative care services: perspectives of patients and nurses. *Int J Palliat Nurs.* 2001;7:171-177.
8. Bestall JC, Ahmed N, Ahmedzai SH, Payne SA, Noble B, Clark D. Access and referral to specialist palliative care: patients' and professionals' experiences. *Int J Palliat Nurs.* 2004;10:381-389.
9. Sano T, Maeyama E, Kawa M, et al. Family caregiver's experiences in caring for a patient with terminal cancer at home in Japan. *Palliat Support Care.* 2007;5:389-395.
10. Japanese EuroQol Translation Team. The development of the Japanese EuroQol instrument. *Health Care Sci.* 1998;8:109-123.
11. Miyashita M, Matoba K, Sasahara T, et al. Reliability and validity of Japanese version STAS (STAS-J). *Palliat Support Care.* 2004;2:379-384.
12. Miaskowski C. New approaches for evaluating the quality of cancer pain management in the outpatient setting. *Pain Manag Nurs.* 2001;2:7-12.
13. Rhodes DJ, Koshy RC, Waterfield WC, Wu AW, Grossman SA. Feasibility of quantitative pain

assessment in outpatient oncology practice. *J Clin Oncol*. 2001;19:501-508.
14. Morita T, Akechi T, Ikenaga M, et al. Late referrals to specialized palliative care service in Japan. *J Clin Oncol*. 2005;23:2637-2644.
15. Kutner JS, Kassner CT, Nowels DE. Symptom burden at the end of life: hospice providers' perceptions. *J Pain Symptom Manage*. 2001;21:473-480.
16. Morita T, Fujimoto K, Tei Y. Palliative care team: the first year audit in Japan. *J Pain Symptom Manage*. 2005; 29:458-465.
17. Tsai JS, Wu CH, Chiu TY, Hu WY, Chen CY. Symptom patterns of advanced cancer patients in a palliative care unit. *Palliat Med*. 2006;20:617-622.
18. Johnson DC, Kassner CT, Houser J, Kutner JS. Barriers to effective symptom management in hospice. *J Pain Symptom Manage*. 2005;29:69-79.
19. Kristjanson LJ, Aoun S. Palliative care for families: remembering the hidden patients. *Can J Psychiatry*. 2004;49:359-365.
20. Hudson P. Home-based support for palliative care families: challenges and recommendations. *Med J Aust*. 2003;179(suppl 6):S35-S37.
21. Harding R, Higginson IJ. What is the best way to help caregivers in cancer and palliative care? A systematic literature review of interventions and their effectiveness. *Palliat Med*. 2003;17:63-74.
22. Stajduhar KI, Davies B. Death at home: challenges for families and directions for the future. *J Palliat Care*. 1998;14:8-14.
23. Nijboer C, Triemstra M, Tempelaar R, Sanderman R, van den Bos GA. Determinants of caregiving experiences and mental health of partners of cancer patients. *Cancer*. 1999;86:577-588.

For reprints and permissions queries, please visit SAGE's Web site at http://www.sagepub.com/journalsPermissions.nav

Loss-of-function *Additional sex combs like 1* mutations disrupt hematopoiesis but do not cause severe myelodysplasia or leukemia

Cynthia L. Fisher,[1,2] Nicolas Pineault,[3,4] Christy Brookes,[1] Cheryl D. Helgason,[3,5] Hideaki Ohta,[3,6] Caroline Bodner,[3] Jay L. Hess,[7] R. Keith Humphries,[3] and Hugh W. Brock[1]

[1]Department of Zoology, University of British Columbia, Vancouver, BC; [2]Wellcome Trust Sanger Institute, Cambridge, United Kingdom; [3]British Columbia Cancer Agency, Vancouver, BC; [4]Héma-Québec, Research and Development Department, Québec, QC; [5]Department of Surgery, Faculty of Medicine, University of British Columbia, Vancouver, BC; [6]Department of Pediatrics, Osaka University Graduate School of Medicine, Osaka, Japan; and [7]Department of Pathology, University of Michigan Ann Arbor

The *Additional sex combs like 1 (Asxl1)* gene is 1 of 3 mammalian homologs of the *Additional sex combs (Asx)* gene of Drosophila. *Asx* is unusual because it is required to maintain both activation and silencing of *Hox* genes in flies and mice. Asxl proteins are characterized by an amino terminal homology domain, by interaction domains for nuclear receptors, and by a C-terminal plant homeodomain protein-protein interaction domain. A recent study of patients with myelodysplastic syndrome (MDS) and chronic myelomonocytic leukemia (CMML) revealed a high incidence of truncation mutations that would delete the PHD domain of *ASXL1*. Here, we show that *Asxl1* is expressed in all hematopoietic cell fractions analyzed. *Asxl1* knockout mice exhibit defects in frequency of differentiation of lymphoid and myeloid progenitors, but not in multipotent progenitors. We do not detect effects on hematopoietic stem cells, or in peripheral blood. Notably, we do not detect severe myelodysplastic phenotypes or leukemia in this loss-of-function model. We conclude that Asxl1 is needed for normal hematopoiesis. The mild phenotypes observed may be because other *Asxl* genes have redundant function with *Asxl1*, or alternatively, MDS or oncogenic phenotypes may result from gain-of-function *Asxl* mutations caused by genomic amplification, gene fusion, or truncation of Asxl1. (Blood. 2010;115: 38-46)

Introduction

Proteins of the Polycomb group (PcG) and trithorax group (trxG) ensure epigenetic maintenance of gene expression patterns through mitosis and faithful propagation of cell fates. PcG genes silence their targets, whereas trxG proteins maintain transcriptional activation. Although the precise mechanism of maintenance is unknown, trxG and PcG genes encode chromatin proteins required for histone modification or establishment or prevention of nucleosome remodeling, or those that enhance or prevent transcriptional elongation.[1] The Enhancer of trithorax and Polycomb (ETP) genes encode proteins required for both maintenance of activation and silencing, as shown by simultaneous anterior and posterior transformations caused by failure to activate or repress *Hox* genes. The molecular basis of ETP function is unknown.[2] Hematopoiesis is a dynamic process requiring coordination between genetic and epigenetic programs to regulate transitions between and maintenance of cell fates, which ultimately generates all blood lineages. Mammalian PcG and trxG genes display hematopoietic lineage- and differentiation stage–specific expression patterns, are required for normal and leukemic hematopoiesis, and show aberrant expression in leukemias and lymphomas.[3-5] Mutations in vertebrate PcG and trxG genes can lead to oncogenic or tumor suppressor activity, depending on context.[3-5]

Additional sex combs like 1 (Asxl1) belongs to the ETP group. Asxl1 regulates *Hox* genes in axial patterning,[6] and is 1 of 3 mammalian homologs of the Drosophila *Asx* gene.[4,5,7-9] As shown in Figure 1A, all mammalian ASXL proteins have conserved sequence features: an amino-terminal ASX homology (ASXH) region, which contains 2 putative nuclear receptor coregulator binding (NR box) motifs, 3 other NR box motifs, and a carboxy-terminal plant homeodomain (PHD) domain.[7,8]

ASXL1 is a member of a repressive complex containing histone H1.2.[9] Conversely, ASXL1 functions autonomously as a transcriptional activator in human cancer cell lines that are retinoic acid (RA) sensitive.[10] ASXL1 enhances recruitment of RA receptors to their chromatin targets, and interacts with the activation domain core of RA receptors in the presence of the ligand RA to increase their activity. However, in other cancer cell lines that are RA resistant, ASXL1 is a corepressor of retinoic acid receptor (RAR) activity.[10] These results support predictions of dual activator/repressor functions for mammalian ASXL proteins depending on cellular context.

ASXL1 is 1 of several fusion protein partners with PAX5 in B-cell precursor acute lymphoblastic leukemia patient samples.[11] A recent study identified ASXL1 mutations in 13% of patients with myelodysplastic syndromes (MDSs) and 43% of patients with chronic myelomonocytic leukemia (CMML).[12] These mutations cause truncation of the protein downstream of the ASXH domain with consequent loss of the PHD domain. These findings suggest that ASXL1 may function as a tumor suppressor in malignancies of the myeloid lineage by affecting stem or progenitor cell self-renewal or differentiation.[12] Recent studies highlight the role of PHD domain mutations or translocations in leukemia,[13] suggesting that the PHD domain of Asxl1 has an important functional role. In

Submitted June 30, 2009; accepted September 29, 2009. Prepublished online as *Blood* First Edition paper, October 27, 2009; DOI 10.1182/blood-2009-07-230698.

The online version of this article contains a data supplement.

The publication costs of this article were defrayed in part by page charge payment. Therefore, and solely to indicate this fact, this article is hereby marked "advertisement" in accordance with 18 USC section 1734.

© 2010 by The American Society of Hematology

this study, we generated a loss-of-function mouse model of *Asxl1* and show that *Asxl1* is required for normal hematopoiesis, but is not required for function of stem cells and multipotent progenitors. Strikingly, these mice did not exhibit MDS or leukemia. These mild phenotypes of *Asxl1* loss-of-function mutations may occur because *Asxl* genes have redundant function, or because *ASXL1* mutations that lead to MDS and CMML are gain of function.

Methods

Gene targeting and generation of *Asxl1*^{tm1Bc} mice

Genomic *Asxl1* fragments from BAC clone no. gs12943 (Genome Systems) and vectors pMTL22[14] and pPNT[15] were used to prepare a replacement targeting vector designed to insert a *PGK* promoter–driven *neomycin* resistance cassette into exon 5 of *Asxl1* at the *Xba*I site (amino acid 90), which is upstream of the conserved ASXH and PHD domains in Asxl1 (Figure 1A-B). The location of the 5′ (at the *Hin*dIII site) and 3′ (at the *Cla*I site) ends of the flanking genomic homology arms in the targeting vector are denoted in larger bold font in Figure 1B. This construct was linearized and electroporated into the E14 mouse embryonic stem cell line, and G418-resistant colonies were selected. All primer sequences are given in supplemental Table 1 (available on the *Blood* website; see the Supplemental Materials link at the top of the online article). Seven of 627 clones were correctly targeted as determined by genomic polymerase chain reaction (PCR) screening using external primer P1 specific for *Asxl1* intron 4, and primer P4 within the neomycin gene (Figure 1B), which yields a 2161-bp PCR product. These were confirmed by Southern blotting. The *neomycin* transgene introduces an additional *Eco*R1 site so that a 3.9-kb fragment is detected when the 5′ external probe (0.5-kb *Eco*R1-*Hin*dIII fragment shown in Figure 1B) is hybridized to *Eco*R1 digested genomic DNA, compared with the 7.3-kb fragment in wild type (Figure 1C). Two independent positive embryonic stem cell clones of normal karyotype were used to inject C57BL/6J blastocysts to generate 2 lines of chimeric mice that were mated to C57BL/6J mice. Chimeras and selected N1 offspring were genotyped by Southern blot and heterozygous mutant mice were backcrossed to C57BL/6J mice. Offspring from N2 or N3 generation *Asxl1*^{tm1Bc} mutant heterozygous parents were used for all experiments reported here, except for the fetal liver competitive repopulation unit (CRU) assay, which used more than N8 generation mice. Adult mice used for experiments ranged in age from 6 to 58 weeks, and at least 1 wild-type littermate control was included for each *Asxl1*^{tm1Bc} mutant sampled concurrently. Genotyping was routinely performed on DNA from adult tail tips, liver from newborns, or yolk sac from embryos, by PCR using primer P2 specific for *Asxl1* intron 4, primer P3 specific for the PGK promoter, and common primer P5 specific for exon 5 downstream of the neomycin cassette. Fragments of 253 bp and 426 bp were indicative of the wild-type and targeted alleles, respectively (Figure 1D). All experiments with animals conformed to the regulations established by the Canadian Council on Animal Care. All protocols were approved by the University of British Columbia Animal Care Committee.

RT-PCR and sequencing of *Asxl1*^{tm1Bc} mRNA

Mouse embryonic fibroblasts (MEFs) were prepared from homozygous mutant E12.5 to E14.5 *Asxl1*^{tm1Bc} embryos, and immortalized by infection with a retroviral vector expressing *Tbx2* as described.[16] RNA was prepared from these MEFs, or from pooled neonate tissues, using Trizol (Invitrogen) and used as templates for cDNA synthesis with poly(dT) and random hexamer primers (Superscript III; Invitrogen). Neonate tissue cDNA was used as a template for PCR reactions under standard conditions with a forward primer from exon 1 and primer P5 or with the exon 1 primer and primer P4. The MEF cDNA was used as a template for PCR reactions with exon 4 and exon 6 primers carried out in the presence of 0.45 M betaine (Sigma). After gel purification, size-selected PCR products were sequenced by the Nucleic Acid Protein Service Unit at the University of British Columbia.

Gene expression analysis

Details on the isolation of murine hematopoietic cell subpopulations by flow cytometry, cDNA generation, global reverse-transcription (RT)–PCR amplification, and gene-specific analysis by Southern blot for actin, *Bmi1*, and *Asxl1* expression are as described.[17] The probe for *Asxl1* was mAsx7A.[8]

Blood and FACS analyses

Peripheral blood of newborn or adult mice was obtained by cardiac puncture immediately after killing. White blood cells were prepared from peripheral blood after incubation in ammonium chloride (StemCell Technologies) to lyse erythrocytes. Cell suspensions of spleen and thymus were prepared using 40-μm nylon mesh strainers. Bone marrow was flushed from both femurs by irrigation of the excised bone using a 22-gauge × 1½ needle and 3-cc syringe and was brought to single-cell suspension by multiple passages through the syringe. Red blood cell and all nucleated cell counts were determined using a hemocytometer.

Single-cell suspensions at a density of 5 to 10 × 10^6 cells/mL were incubated on ice, protected from light, for 30 to 60 minutes, and were singly, doubly, or triply stained with specific monoclonal antibodies to the murine cell surface antigens: Gr-1 (Ly-6G) and Mac-1 (CD11b) monocyte and granulocyte markers; Ter-119 (Ly-76) erythroid lineage marker; CD4 (L3T4), CD8a (Ly-2), CD44 (Pgp-1, Ly-24), and CD25 (interleukin-2 [IL-2] receptor chain α) T-lymphoid lineage markers; B220 (CD45R), CD43 (Ly-48, leukosialin), surface immunoglobulin M (IgM; R6-60.2), and surface IgD B-lymphoid lineage markers; and Ly5.2 mouse strain–specific marker. The antibodies were conjugated to the fluorochromes fluorescein isothiocyanate (FITC) or phycoerythrin (PE) as indicated in the figures. All antibodies were from BD PharMingen, except for the anti-IgD antibody, which was from Southern Biotech Associates Inc. Cell sorting was performed on FACSCalibur, FACScan, or FACSort flow cytometers (Becton Dickinson). Dead cells were excluded from analysis using forward and side scatter and phosphatidyl inositol staining. Acquisition and analysis were performed with CELLQuest software (Becton Dickinson).

Clonogenic progenitor assays

To detect multipotential myeloid lineage clonogenic progenitors 2.5 × 10^4 cells from embryonic day (E) 18.5 fetal liver, newborn spleen, or adult bone marrow were plated in a 1.1-mL volume per Greiner Petri dish. Cells were plated in Methocult M3434 methylcellulose medium (StemCell Technologies) containing 10 ng/mL recombinant murine IL-3, 10 ng/mL recombinant human IL-6, 50 ng/mL recombinant murine steel factor, and 3 U/mL recombinant human erythropoietin. Myeloid and erythroid cell colonies were counted and scored after 10 to 12 days. To detect pre-B-lymphoid clonogenic progenitors, 1.0 × 10^5 cells from adult bone marrow were plated in a 1.1-mL volume per Greiner Petri dish in Methocult M3630 methylcellulose medium (StemCell Technologies) containing 10 ng/mL IL-7.[18] The number of B-cell colonies was scored after 5 to 7 days. All cell culture was performed in a humidified incubator at 37°C at 5% CO_2. All colonies were scored microscopically using standard phenotypic criteria. Final colony-forming unit (CFU) values represent the average of 2 replicates per sample.

Fetal thymic organ culture

Fetal thymus lobes were dissected from E14.5 embryos and cultured as described.[19] Thymocytes were stained with monoclonal antibodies against CD4 and CD8, and analyzed by fluorescence-activated cell sorting (FACS) as described in "Blood and FACS analyses."

Day-12 CFU-S and competitive repopulating unit assay

Methods used for the day-12 spleen colony-forming unit (CFU-S_{12}) and competitive repopulation unit (CRU) assays are as previously described.[20] Reconstitution was tested at 11 and 20 weeks after transplant by FACS analysis to detect Ly5.2 and B220, CD4 and CD8, or Gr1 and Mac1, from peripheral blood from the tail vein. Mice whose blood contained greater than 1% donor-derived (Ly5.2$^+$) myeloid cells (Gr-1$^+$ and/or Mac-1$^+$), B cells (B220$^+$), and T cells (CD4$^+$ and/or CD8$^+$) were considered to have

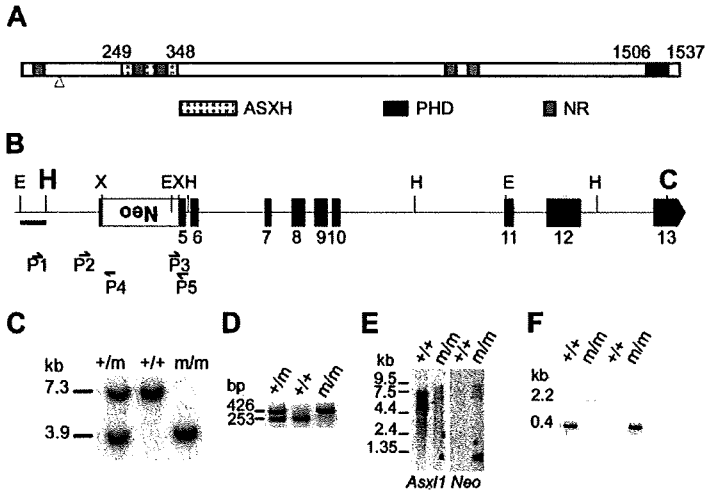

Figure 1. Generation of *Asxl1* mutant mice. (A) Schematic representation of the conserved ASXH and PHD domains and NR sequence motifs in ASXL1 homologs is shown.[8] Numbers above the diagram show the first and last amino acids that define the ASXH and PHD domains. Mutations causing ASXL1 truncations found in MDS and CMML patients lie between amino acids 596 and 1457, all within exon 12.[12] The arrowhead shows the site of insertion of the *neomycin* (neo) transgene at amino acid 90. (B) Diagram of part of the *Asxl1* locus showing exons 5 to 13 indicated as black boxes. The PGKneo expression cassette (large white box) was inserted into the *Xba*I site in exon 5 by a replacement gene-targeting approach and was used for positive selection of clones. Position of relevant restriction sites (C indicates *Cla*I; E, *Eco*RI; H, *Hin*dIII; and X, *Xba*I), the location of external probe (bar below the E-H fragment shown at the left), and PCR primers (small arrows) are indicated. The location of the 5′ (*Hin*dIII site) and 3′ (*Cla*I site) ends of the flanking genomic homology arms in the targeting vector is denoted in larger bold font. (C) Southern blot analysis of genomic DNA isolated from newborn offspring of an $Asxl1^{tm1Bc}$ intercross after digestion with *Eco*RI and hybridized with an external probe shown in panel B. This probe detects a 7.3-kb fragment from the wild-type allele (+/+), and a 3.9-kb fragment from the targeted allele (m/m). (D) Multiple primer PCR analysis of liver genomic DNA of E18.5 embryos from an $Asxl1^{tm1Bc}$ intercross. Primers P2 and P5 amplify a 253-bp fragment of the wild-type allele, whereas primers P3 and P5 amplify a 426-bp fragment of the targeted allele. (E) Northern blot analysis of poly(A)$^+$RNA from pooled tissue of neonate wild-type and $Asxl1^{tm1Bc}$ mice using probes for *Asxl1* (left panel) and neomycin (right panel). (F) RT-PCR analysis of $Asxl1^{tm1Bc}$ mutant neonate tissue. RT-PCR of total RNA from pooled tissue of individual newborn $Asxl1^{+/+}$ (+/+) and $Asxl1^{tm1Bc/tm1Bc}$ (m/m) mice. Primer from exon 1 and primer P5 (in exon 5) amplify an approximately 400-bp product in $Asxl1^{+/+}$ samples, and a 2.2-kb product in $Asxl1^{tm1Bc/tm1Bc}$ (left panel). Primer from exon 1 and primer P4 (within neo) amplify a 300-bp product from the $Asxl1^{tm1Bc/tm1Bc}$ samples, whereas no amplification occurs in the $Asxl1^{+/+}$ samples, as expected (right panel).

been repopulated with transduced cells. CRU frequencies in the test fetal liver samples were calculated by applying Poisson statistics to the proportion of negative recipients at different dilutions using L-Calc (StemCell Technologies) software.

Statistical analyses

Comparison of means between groups was done using the Student *t* test. Differences with *P* values less than .05 were considered statistically significant.

Results

Generation of $Asxl1^{tm1Bc}$ mutant mice

The *Asxl1* gene was disrupted using targeted replacement mutagenesis by permanent insertion of a PGK promoter–driven neomycin-resistance (neo) gene in reverse orientation to the *Asxl1* direction of transcription into the *Xba*I site of exon 5 (Figure 1B; see "Gene targeting and generation of $Asxl1^{tm1Bc}$ mice" for details and controls). This insertion interrupts the reading frame of *Asxl1* by introducing several premature termination codons after the corresponding amino acid 90 position, upstream of the conserved ASXH domain (Figure 1A).[8] To determine whether *Asxl1* mRNAs containing the transgene were expressed, we performed Northern blots to show that all detectable transcripts in $Asxl1^{tm1Bc/tm1Bc}$ mutant embryos contain the transgene and to confirm neomycin expression (Figure 1E). It is likely these *Asxl1* mutant transcripts are not transcribed due to nonsense-mediated decay, however any stable truncated protein generated from these mRNAs would lack the conserved ASXH and PHD domains and all NR box motifs except one at the extreme amino-terminus (Figure 1A),[8] and likely would be nonfunctional.

We generated a polyclonal antibody against amino acids 811 to 929 of Asxl1, but we were unable to detect endogenous Asxl1 protein expression in Western blots of MEFs (data not shown). We therefore performed RT-PCR on $Asxl1^{tm1Bc}$ mutant tissues and embryonic fibroblast (MEF) lines, to confirm the predicted transcript structure, and to assess whether use of cryptic splice sites resulted in the generation of aberrant splice variants from the mutated *Asxl1* allele that may be translated. PCR with the exon 1 primer and primer P5 amplifies an approximately 400-bp band in $Asxl1^{+/+}$ samples, and a 2.2-kb band in $Asxl1^{tm1Bc/tm1Bc}$ samples consistent with read-through of the inserted PGKneo cassette (Figure 1F). The exon 1 primer and primer P4 amplify a band from the $Asxl1^{tm1Bc/tm1Bc}$ samples, confirming expected reverse orientation of the neo cassette, whereas no amplification occurs in the $Asxl1^{+/+}$ samples (Figure 1F). We performed PCR with primers from exon 4 and exon 6 that flank the insertion site of the targeting cassette in exon 5. Sequencing of the product showed that an abnormal splicing event in $Asxl1^{tm1Bc}$ mutants can remove all of exon 5, including the targeting cassette, from a minority of the transcripts (supplemental Figure 1). This abnormally spliced $Asxl1^{tm1Bc}$ mRNA would have an altered reading frame with premature termination codons and would likely undergo nonsense-mediated decay. We therefore predict that the $Asxl1^{tm1Bc}$ mutant allele is a null allele. The $Asxl1^{tm1Bc}$ mutant mice exhibit partially penetrant perinatal lethality, and show developmental phenotypes consistent with Enhancer of trithorax and Polycomb (ETP) function, as described in detail elsewhere.[6]

Asxl1 is expressed ubiquitously in hematopoietic cells

To assess *Asxl1* expression in hematopoietic cells, we used global cDNA amplification of hematopoietic cells fractionated by FACS

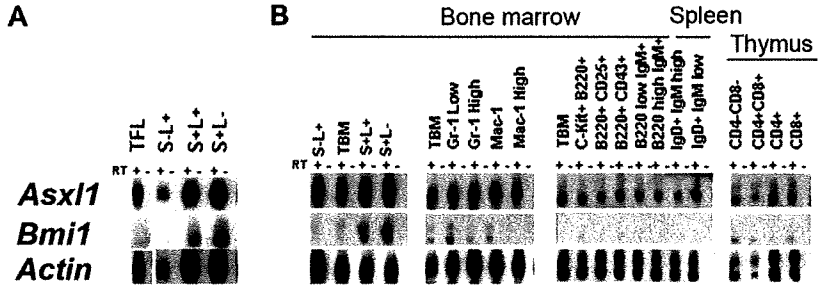

Figure 2. *Asxl1* is ubiquitously expressed in hematopoietic cells. Southern blot analysis of *Asxl1*, *Bmi1*, and *actin* gene expression in total amplified cDNAs from FACS-sorted hematopoietic cell populations from fetal liver and adult bone marrow, spleen, and thymus. Total cDNAs were amplified using RT-PCR from 10^4 sorted cells, and each sample with or without reverse transcriptase (RT + or −) was sequentially hybridized to each probe. Results for a representative experiment are shown; duplicate experiments were performed. (A) *Asxl1* is expressed in unfractionated E14.5 fetal liver (TFL), and the hematopoietic stem cell–depleted (Sca-1$^-$Lin$^+$ [S$^-$L$^+$]), low (Sca-1$^+$Lin$^+$ [S$^+$L$^+$]), and enriched (Sca-1$^+$Lin$^-$ [S$^+$L$^-$]) subpopulations, whereas *Bmi1* expression is predominant in the 2 Sca-1$^+$ fractions. (B) *Asxl1* is expressed in unfractionated adult bone marrow (TBM) and in all fractionated adult bone marrow, spleen, and thymus cells investigated, whereas *Bmi1* is expressed predominantly within the progenitor-enriched Sca-1$^+$ fractions and the Gr-1 low fraction of total bone marrow, with very low or undetectable expression in other fractions.

into hematopoietic stem cells (HSCs) and primitive clonogenic, pluripotent progenitors and mature cells, followed by Southern blot analysis using gene-specific probes as described.[17] *Asxl1* is expressed ubiquitously in all progenitor-enriched and mature hematopoietic cell–enriched fractions analyzed in fetal liver (Figure 2A) and adult bone marrow (Figure 2B). *Asxl1* expression is ubiquitous in mature myeloid cells (monocytes/macrophages [Mac-1$^+$] and granulocytes [Gr-1$^+$]), in lymphoid lineages, including FACS fractionated cells from adult bone marrow enriched for B-cell progenitors (cKit$^+$B220$^+$, B220$^+$CD25$^+$, B220$^+$CD43$^+$) or immature B cells (B220$^+$IgM$^+$), in mature spleen-derived B cells (IgD$^+$IgM$^+$; Figure 2A), and in all fractionated CD4 CD8 subpopulations representing the major stages of T-lymphoid cell differentiation obtained from adult thymus. In contrast, the expression of *Bmi1* is highest in progenitor-enriched Sca$^+$Lin$^-$ and Sca$^+$Lin$^+$ fractions, whereas expression was low to undetectable in all other fractions analyzed (Figure 2).

Effects of *Asxl1^{tm1Bc}* mutation on T lymphopoiesis

Thymus cellularity of *Asxl1^{tm1Bc}* mutant mice older than 15 weeks was drastically decreased compared with *Asxl1$^{+/+}$* controls, and so we grouped mice according to age for further analysis (Figure 3A). There is a relative increase in the number of double-negative (CD4$^-$CD8$^-$) thymocytes in *Asxl1^{tm1Bc}* mutant compared with control thymi (Figure 3B). When the overall reduction in thymus cellularity of older mutant *Asxl1^{tm1Bc}* mice is taken into account, all CD4 CD8 subcompartments show a significant reduction in absolute cell number (Figure 3C). However, there were no significant differences in the absolute numbers of single-positive (CD4$^+$ or CD8$^+$) or double-positive (CD4$^+$CD8$^+$) cells in the peripheral blood (supplemental Figure 2).

To determine whether defects in thymopoiesis could be detected earlier in development, we used the fetal thymic organ culture assay to measure relative proportions of CD4- and CD8-expressing T cells from E14.5 thymi. We detected no significant differences in the relative proportion of double-negative, double-positive, or CD8 single-positive populations. However there was a modest decrease in the proportion of CD4 single-positive cells from *Asxl1$^{tm1Bc/tm1Bc}$* embryos compared with wild-type littermate-derived samples (Figure 4).

Effects of *Asxl1^{tm1Bc}* mutation on B lymphopoiesis

There was no effect of the *Asxl1^{tm1Bc}* mutation on E18.5 fetal liver cellularity, or adult bone marrow cellularity, regardless of age (supplemental Figure 3). However, a subset of *Asxl1^{tm1Bc}* mutant mice older than 15 weeks showed a relative decrease in B-lymphoid cell numbers within peripheral blood, spleen, and bone marrow, as illustrated by reduced expression of the pan-B-cell marker B220 and the mature B-cell markers IgM and IgD, compared with littermate wild-type controls (Figure 5A; severe case shown). Absolute numbers of B220$^+$ cells, B220$^+$IgM$^+$ immature B cells, and IgM$^+$IgD$^+$ mature B cells were significantly reduced in bone marrow of mice older than 15 weeks (Figure 5B and supplemental Figure 3), whereas a modest though not statistically significant decrease was seen in bone marrow of mice younger than 15 weeks (supplemental Figure 3A) and in spleen (Figure 5C). However, no significant difference in absolute number of B220$^+$ and IgM$^+$IgD$^+$ cells was seen in the peripheral blood (supplemental Figure 2), suggesting highly variable penetrance of the effect on B cells of *Asxl1^{tm1Bc}* mice compared with wild-type controls. To determine whether there was a reduction in the number of pro-B precursor cells in *Asxl1$^{tm1Bc/tm1Bc}$* bone marrow, we monitored coexpression of B220 and CD43 using flow cytometry. Overall, the differences between *Asxl1$^{tm1Bc/tm1Bc}$* and *Asxl1$^{+/+}$* control samples were not statistically significant (Figure 5B). This suggests that the major defect in B-cell progression for most *Asxl1$^{tm1Bc/tm1Bc}$* mice occurred after pro-B differentiation. To determine whether *Asxl1^{tm1Bc}* mutation affected progression through the IL-7–responsive, pre-B progenitor stage, we analyzed bone marrow from adult *Asxl1$^{tm1Bc/tm1Bc}$* mice (all older than 12 weeks) in a CFU–IL-7 methylcellulose colony assay. There were severe reductions in the frequency of CFU–IL-7 generated from the *Asxl1$^{tm1Bc/tm1Bc}$* bone marrow samples compared with wild-type controls (Figure 5D), consistent with an impaired transition to the pre-B stage.

Effects of *Asxl1^{tm1Bc}* mutation on erythropoiesis and myelopoiesis

We analyzed properties of hematopoietic cells from homozygous *Asxl1^{tm1Bc}* mice at stages E18.5, P1, and adult (> P42). P1 and adult *Asxl1^{tm1Bc}* homozygous null mutants showed no differences in peripheral blood red or white cell counts compared with *Asxl1$^{+/+}$*, regardless of whether they were grouped according to age as described in the previous section (supplemental Figure 4). We did not observe any significant changes in platelets, erythrocyte, leukocyte, or thrombocyte morphology, by visual examination of Wright-Giemsa–stained blood smears or changes in cell morphology in cytospin preparations of spleen and bone marrow cells of *Asxl1^{tm1Bc}* mutants compared with wild-type controls (data not shown).

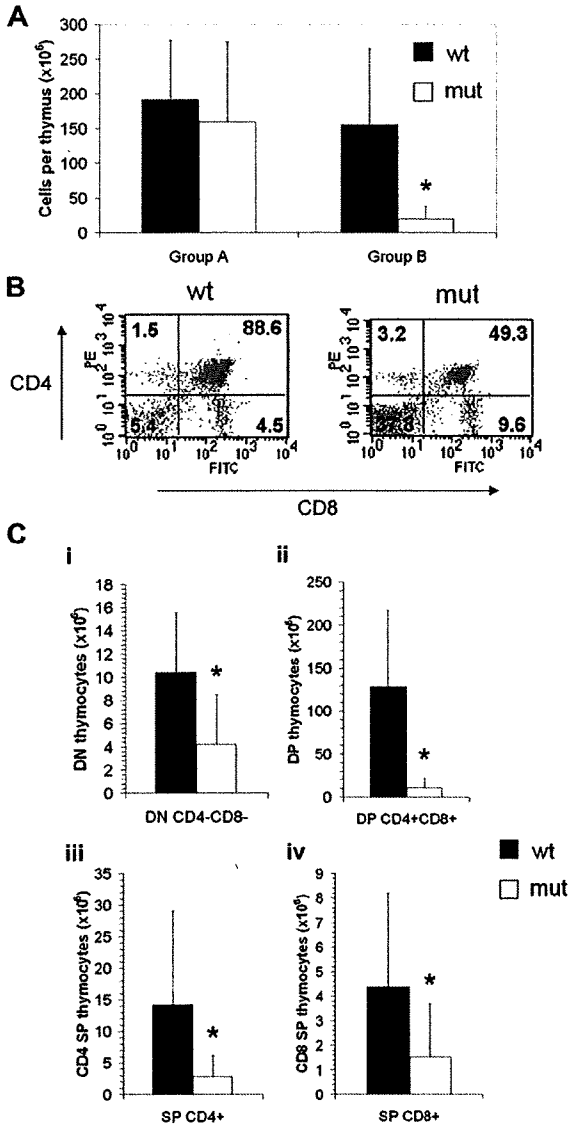

Figure 3. *Asxl1*$^{tm1Bc/tm1Bc}$ mutant mice exhibit reduced thymopoiesis. (A) Thymus cellularity is reduced in older (older than 15 weeks; group B, n = 8 each genotype) compared with younger (15 weeks or younger; group A, n = 6 wt, 4 mutant) *Asxl1*$^{tm1Bc/tm1Bc}$ (mut) adult mice compared with wild type. (B) Flow cytometry of T lymphocytes from adult thymus expressing the lineage markers CD4 and CD8 shows a relative increase in the double-negative and both single-positive fractions, and a relative decrease in the double-positive fraction in *Asxl1*$^{tm1Bc/tm1Bc}$ thymus compared with wild type. (C) Absolute cell number per thymus is reduced in group B *Asxl1*$^{tm1Bc/tm1Bc}$ mice compared with wild type for all fractions: (i) double-negative CD4$^-$CD8$^-$ (DN), (ii) double-positive CD4$^+$CD8$^+$ (DP), (iii) single-positive (SP) CD4$^+$, and (iv) single-positive CD8$^+$ (n = 8). *$P < .05$.

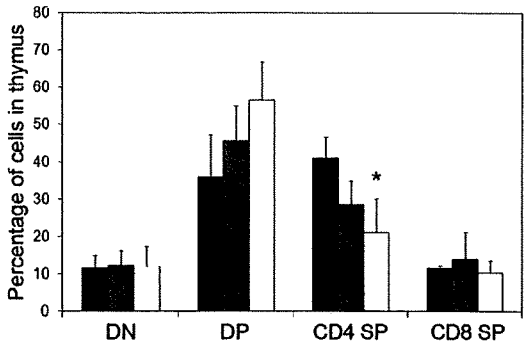

Figure 4. Flow cytometric analysis of T cells cultured from E14.5 thymus. Cells were analyzed using monoclonal antibodies against CD4 and CD8. Numbers indicate the percentage of cells within each subcompartment: double-negative CD4$^-$CD8$^-$ (DN), double-positive CD4$^+$CD8$^+$ (DP), single-positive CD4 (CD4$^+$SP), and single-positive CD8 (CD8$^+$SP). *$P < .05$. ■ indicates wild type (n = 2); ▨, *Asxl1*$^{+/tm1Bc}$ (n = 6); and □, *Asxl1*$^{tm1Bc/tm1Bc}$ mutant (n = 7).

The *Asxl1*^{tm1Bc} mutation had modest and variable effects on myelopoiesis. Consistent with increased splenic cellularity of a subset of adult mice (Figure 6A), a significant increase in *Asxl1*^{tm1Bc} adult splenocytes expressing Gr-1 and Mac-1 was observed (Figure 6B-C). Sections of adult *Asxl1*^{tm1Bc} showed normal morphology with prominent extramedullary hematopoiesis present within the red pulp regions of the enlarged *Asxl1* mutant spleens (not shown). Cellularity and histology of P1 spleens was normal (not shown). We conducted in vitro colony assays of E18.5 fetal liver, P1 spleen, and adult bone marrow cells, grown in methylcellulose and supplemented with growth factors that support CFU-C myeloerythroid lineage multipotential and unipotential progenitor differentiation (Figure 7). Overall, there is a slight reduction in myeloerythroid colony-forming ability across the colony types scored: granulocyte-macrophage (GM), and granulocyte-erythrocyte-macrophage-megakaryocyte (GEMM). Statistically significant reductions in colony number were seen only for E18.5 fetal liver GM and total CFU-C myeloid, and newborn spleen GEMM ($P < .05$). No significant changes in the percentages of myeloid cells were observed in adult peripheral blood (supplemental Figure 2) or bone marrow (not shown).

Effects of *Asxl1*^{tm1Bc} mutation on progenitor and hematopoietic stem cell activity

Because we observed *Asxl1* expression in cell fractions enriched for hematopoietic progenitors and HSC in fetal liver and adult bone marrow (Figure 2), we assessed the functional requirement for Asxl1 in these cells using the day-12 spleen colony-forming unit (CFU-S_{12}) assay.[21] In 2 independent experiments, we found no differences in CFU-S_{12} colony numbers between *Asxl1* mutant and control samples within either experiment (data not shown).

To assess whether the *Asxl1*^{tm1Bc} mutation affected function of long-term repopulating HSCs, we carried out a standard competitive repopulation unit (CRU) assay in which various numbers of either wild-type or homozygous *Asxl1*$^{tm1Bc/tm1Bc}$;Ly5.2$^+$ cells derived from E17 fetal liver were injected into Ly5.1$^+$ congenic irradiated hosts in the presence of helper Ly5.2$^+$ wild-type cells. We observed no significant difference in CRU frequency, based on FACS immunophenotyping of peripheral blood, between recipients of *Asxl1*^{tm1Bc} mutant and *Asxl1*$^{+/+}$ cells in this assay, at 20 weeks after transplant (data not shown).

Discussion

We generated a knockout mouse model of the ETP group gene *Asxl1* to assess the effect of loss of function of Asxl1 in hematopoiesis. The *Asxl1*^{tm1Bc} mutation had consistent and profound effects on lymphopoiesis. The data suggest that the T-lymphopoiesis defect in the *Asxl1*^{tm1Bc} mutants lies in the DN1 to DN4 precursor stage.[18] *Asxl1*^{tm1Bc} mice also exhibited striking defects in B lymphopoiesis at the progenitor level. The number of bone marrow pre-B progenitor cells detectable by the CFU–IL-7 in vitro assay is markedly lower in all samples from *Asxl1*$^{tm1Bc/tm1Bc}$ adult mice compared with wild-type controls, consistent with the

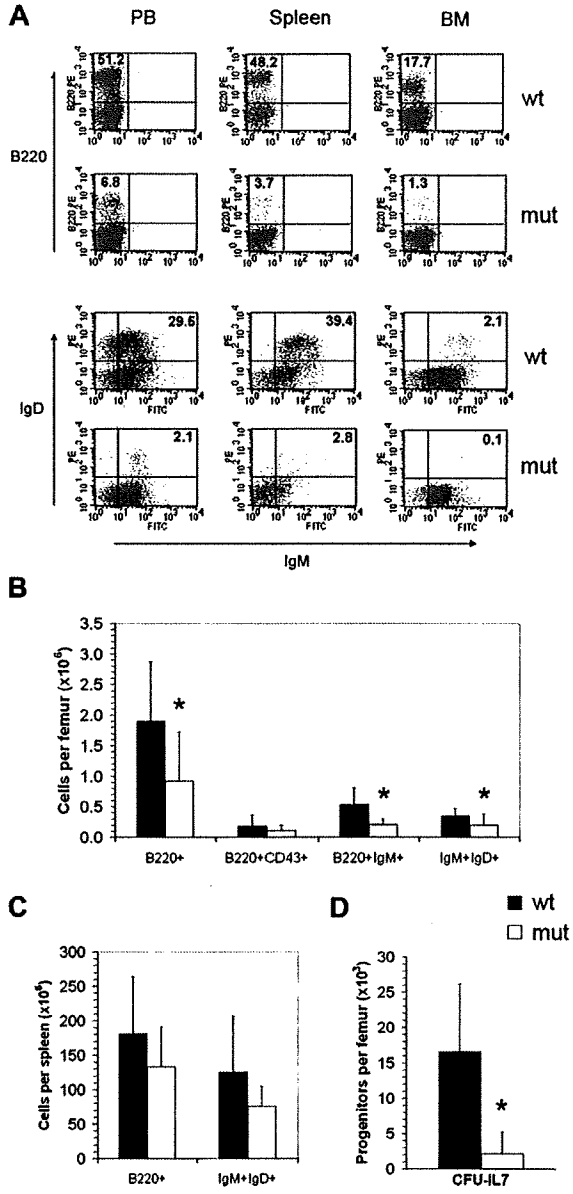

Figure 5. *Asxl1*$^{tm1Bc/tm1Bc}$ mutant mice exhibit reduced B-cell lymphopoiesis. (A) Flow cytometric profiles of adult (> 15 weeks old) peripheral blood (PB), spleen, and bone marrow (BM) show a relative decrease in B220- and IgM/IgD-positive cells in *Asxl1*$^{tm1Bc/tm1Bc}$ (mut) tissues compared with wild type (wt). (B) Absolute bone marrow cell numbers in adult femur expressing the markers B220; B220 and CD43; B220 and IgM; and IgM and IgD are significantly lower in *Asxl1*$^{tm1Bc/tm1Bc}$ mice compared with wild type (n = 8 each genotype except n = 4 for B220 and IgM). (C) Absolute cell numbers from > 15-week-old spleen expressing the markers B220, and IgM and IgD, are lower in *Asxl1*$^{tm1Bc/tm1Bc}$ mice compared with wild type (n = 8 each genotype). (D) In vitro colony formation of committed pre-B-lymphocyte progenitors (CFU-IL-7 assay) from adult bone marrow (> 15 weeks old) is significantly reduced in cultures of *Asxl1*$^{tm1Bc/tm1Bc}$ group B compared with wild type (n = 7 wt, 8 mutant). *$P < .05$.

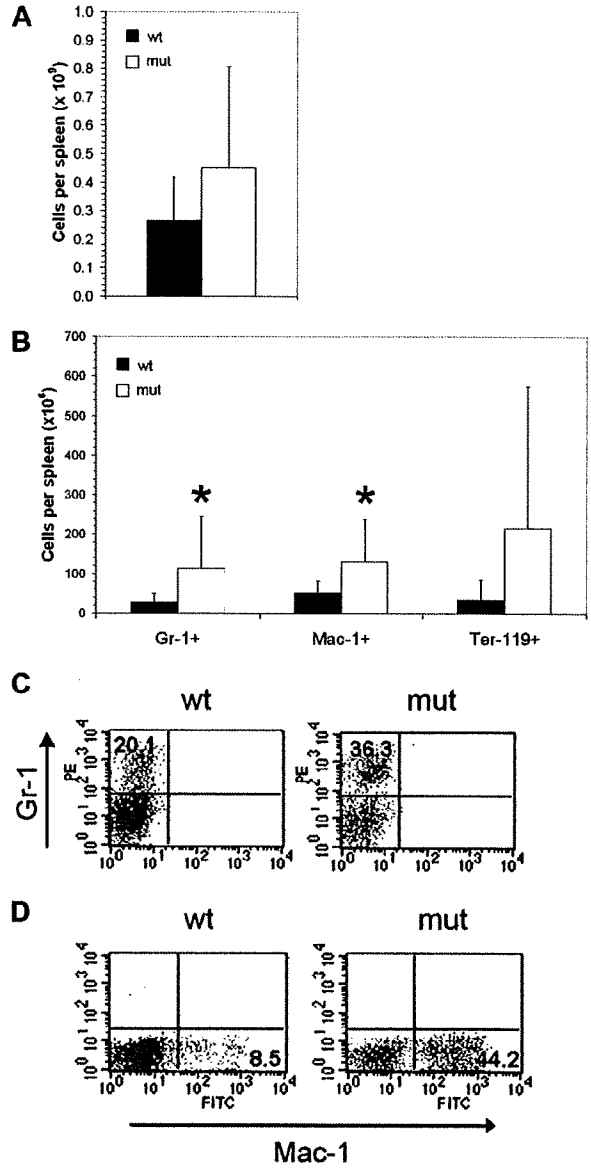

Figure 6. *Asxl1*$^{tm1Bc/tm1Bc}$ mutant mice exhibit splenomegaly and increase in myeloid cell number. (A) Cellularity of *Asxl1*$^{tm1Bc/tm1Bc}$ (mut) adult spleens is increased compared with wild type (wt; n = 14 wt, 12 mutant). (B) In adult *Asxl1*$^{tm1Bc/tm1Bc}$ mice, the absolute numbers of myeloid (Gr1 or Mac1 positive) and erythroid (Ter119 positive) cells are increased in spleen (Gr1$^+$ n = 13 wt, 11 mutant; Mac1$^+$ n = 11; Ter119$^+$ n = 10 wt, 7 mutant). (C) The proportion of cells bearing the myeloid lineage markers Gr1 (i) and Mac (ii) is increased in adult spleen of *Asxl1*$^{tm1Bc/tm1Bc}$ mutants.

lower absolute number of B220$^+$ cells within the bone marrow of most adult *Asxl1*$^{tm1Bc/tm1Bc}$ mice. Of note, defective B-lymphoid development is seen in mice mutant for other PcG genes.[19,22-27]

Our data suggest that there is a progressive collapse of the lymphoid compartment in *Asxl1*^{tm1Bc} mutant mice over time, because both T- and B-lymphoid defects were observed in mutant mice greater than 15 weeks of age but not in younger mice. However, as the experiments we conducted were not specifically designed to evaluate the timing of phenotypic changes, we cannot adequately address onset and progression of the defects in lymphopoiesis from our current study. This should be carefully assessed in future studies, which would ideally be conducted using a conditional mouse mutant model to specifically ablate Asxl1 in hematopoietic cells, and would also avoid problems associated with partial perinatal lethality of the constitutive *Asxl1* null mice.

It is interesting to note that the reduced thymopoiesis observed in loss-of-function *Hoxa9* mouse mutants ameliorates with age[28] in contrast to the increase in severity of thymic defects observed in *Asxl1* mutants. We report elsewhere[6] that *Asxl1* mutations cause misexpression of *Hox* genes in mesodermal derivatives during embryonic development. It may be that in the absence of Asxl1,

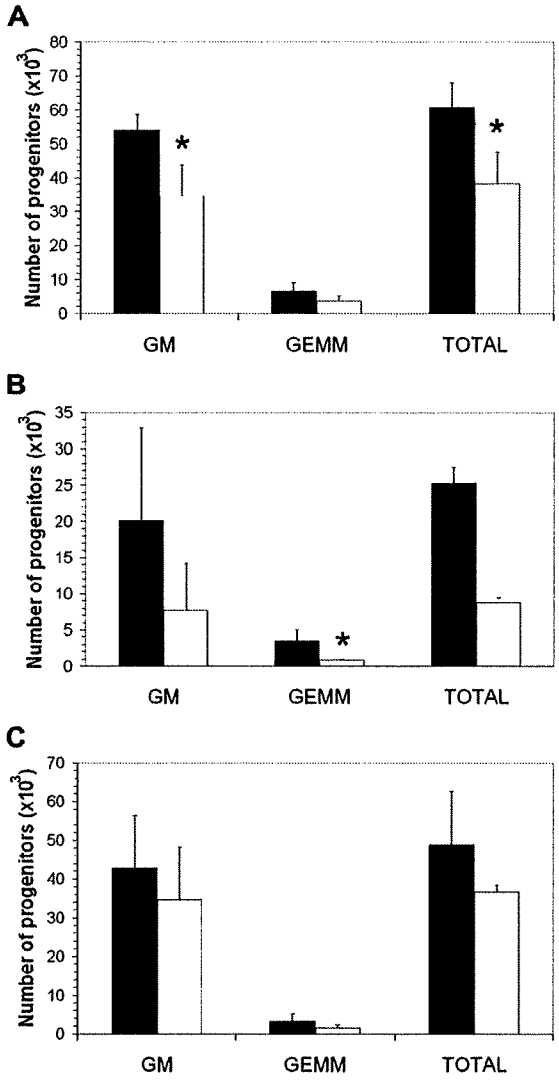

Figure 7. *Asxl1*$^{tm1Bc/tm1Bc}$ mutant mice have fewer committed myeloerythroid progenitors. In vitro colony formation of committed myeloerythroid progenitors (CFU-GEMM assay) is reduced in *Asxl1*$^{tm1Bc/tm1Bc}$ mice compared with wild type in cultures of (A) E18.5 fetal liver (n = 2 wt, 3 mutant), (B) newborn spleen (n = 6 wt, 5 mutant), and (C) adult bone marrow (n = 9 wt, 6 mutant) *$P < .05$. ■ indicates wild type; □, *Asxl1*$^{tm1Bc/tm1Bc}$ mutant.

aberrant expression of *Hoxa9*, or other *Hox* genes that have a known role in regulation of hematopoiesis, leads to the thymic defects seen in *Asxl1* mutants.[29] However not all hematopoietic defects seen in PcG mutants are a consequence of Hox gene misregulation, as evidence from *Rae28* and *eed* mutant mice indicates that defects in fetal liver and adult hematopoiesis, respectively, are not mediated via *Hox* targets.[30,31] Conversely, certain *Hox* genes do play a critical role in leukemogenesis involving the trithorax gene *Mll*, as *Hoxa7* and *Hoxa9* are required for myeloid transformation mediated by Mll chimeric fusion proteins,[32] and are also likely regulated by Mll during normal hematopoiesis because down-regulation of *Hoxa7*, *Hoxa9*, and *Hoxa10* was observed in E12.5 fetal liver of *Mll* homozygous mutant mice.[33]

Myeloerythroid lineage defects in *Asxl1*^{tm1Bc} mutants are mild. This is consistent with observations that other PcG and trxG genes exhibit variable effects on myeloerythropoiesis and erythropoiesis.[22,24,26,34-41] *Bmi1*, *Phc1*, and *Mll1* mutations that affect myeloerythropoiesis may do so indirectly by negatively affecting HSC activity, resulting in reduced differentiation along all hematopoietic lineages,[20,25,42-44] but this possibility is unlikely for *Asxl1* as we did not observe effects on HSCs or multipotent progenitors.

Despite the observation of changes in cell frequency in liver, spleen, thymus, and bone marrow, mature hematopoietic cell types exhibiting normal morphology and number were observed within the peripheral blood of most adult *Asxl1*$^{tm1Bc/tm1Bc}$ mice. These results suggest that in the absence of Asxl1, homeostatic compensatory mechanisms normalize myeloid, erythroid, and lymphoid cells despite disturbances in progenitor cells, consistent with previous studies of Polycomb and trithorax group mutants.[26,27,34-36,40]

Many Polycomb and trithorax group mutants affect self-renewal of HSCs.[34-37,42-45] However, *Asxl1*^{tm1Bc} fetal liver reconstituted all blood lineages in irradiated adult mice up to 20 weeks in a competitive repopulation assay and the *Asxl1*^{tm1Bc} mutation does not alter colony numbers in the CFU-S_{12} assay.[21] Therefore Asxl1 is not required for HSC or multipotent progenitor activity. However, the in vitro clonogenic progenitor assays show a modest reduction in CFU-GEMM activity in *Asxl1* mutants, indicating a possible role in common myeloid progenitor regulation. Serial transplant assays with *Asxl1* mutant cells may reveal more progressive defects at the HSC level such as were seen in studies of the Polycomb group gene *Phc1*^{tm1Cs} mutant mice.[20]

The failure to observe lymphomas or leukemias in *Asxl1*$^{tm1Bc/tm1Bc}$ mutant mice monitored for up to 58 weeks suggests that loss of Asxl1 alone is insufficient to cause oncogenic transformation. In light of a recent study characterizing mutations in the human ASXL1 gene in bone marrow samples from patients with MDS and CMML,[12] it is perhaps surprising that our investigations of loss-of-function *Asxl1* mutant mice did not reveal more profound defects in HSC or progenitor function with respect to myelopoiesis, and that the mice did not develop myelodysplastic phenotypes other than splenomegaly. One explanation is that *Asxl1*, *Asxl2*, and perhaps *Asxl3* have redundant functions in hematopoiesis. This idea is supported by observations that deletions of *Asxl2*[12] and an *ASXL2-MOZ* fusion (GenBank accession number AB084281[46]) are also associated with MDS. Furthermore, the chromosomal region at 2p23, the site of *ASXL2*, is amplified in a variety of tumor types, including B-cell leukemia and lymphomas.[47]

Another potential explanation for the mild phenotypes of loss-of-function *Asxl1* mutations stems from the observation that mutations found in the MDS and CMML samples were all found in exon 12 and spanned the region from Arg596 to Ser1457 of the corresponding 1541 amino acid ASXL1 protein (Figure 1).[12] These mutations would remove the C-terminal PHD domain but leave the N-terminal ASXH region containing 2 putative NR box motifs, and all putative nuclear localization signal sequences intact.[7,8] These ASXL1 truncations may function as dominant negative mutations, leading to a more severe phenotype compared with the null mutation described here, which removes both the ASXH and the PHD domains. Loss-of-function *ASXL1* mutations have not yet been associated with cancer to our knowledge. Interestingly, oncogenic effects of *ASXL1* mutations are associated with gain-of-function *ASXL1* mutations, consistent with overexpression of *ASXL1* in cancer cell lines,[7] with amplification of region 20q11.21 that contains the *ASXL1* locus in a wide range of human tumors,[48-51] and with the *PAX5-ASXL1* fusions detected previously in acute lymphoblastic leukemia patients.[11]

ASXL1 functions as a nuclear receptor coregulator in human cancer cell lines.[10] In transfected HeLa cells stably expressing a

FLAG-ASXL1 construct, there was a striking increase in RA-dependent RAR-induced transcription, whereas in cells expressing a truncated form of ASXL1 lacking the PHD domain, there was only a slight enhancement of RAR activity, suggesting that the PHD domain mediates nuclear receptor activity.[10] RA is a well-established therapeutic agent for acute promyelocytic leukemia.[52] Perhaps aberrant RA receptor signaling in cells with truncation of the PHD domain of ASXL1 may contribute to development of dysplasia if RA cytotoxicity is enhanced in cells overexpressing ASXL1 truncations.[10]

Acknowledgments

We thank Rewa Grewal, Carolyn Bateman, Pol Gomez, and Gosta Berg for technical assistance.

This research was supported by grants from the Canadian Institutes of Health Research to H.W.B., from the Terry Fox Foundation to R.K.H., and from the National Institutes of Health (RO1-CA-0078815) and a SCOR grant from the Leukemia & Lymphoma Society of America to J.L.H. C.L.F. was supported by a Medical Research Council of Canada studentship. C.D.H. was supported by a Canadian Institutes of Health Research New Investigator award, and is a Michael Smith Foundation for Health Research scholar.

Authorship

Contribution: C.L.F., N.P., C.D.H., H.O., R.K.H., and H.W.B. designed experiments; N.P. analyzed *Asxl1* expression; C.L.F. constructed the *Asxl1* targeting vector; C.D.H. and C. Bodner performed embryonic stem cell tissue culture; C.L.F. performed genotyping assays; C.L.F. with assistance from C.D.H. and C. Bodner performed FACS immunophenotyping, in vitro functional assays, and general hematopoietic analysis in *Asxl1* mutants; H.O. performed the thymic organ culture experiments; C. Brookes carried out the competitive repopulation assays; J.L.H. carried out pathologic examinations; C.L.F., R.K.H., and H.W.B. wrote the manuscript; and C.D.H., N.P., H.O., and J.L.H. suggested improvements to the manuscript.

Conflict-of-interest disclosure: The authors declare no competing financial interests.

Correspondence: Hugh W. Brock, Department of Zoology, University of British Columbia, 2350 Health Sciences Mall, Vancouver, V6T 1Z3, BC Canada; e-mail: brock@zoology.ubc.ca.

References

1. Brock HW, Fisher CL. Maintenance of gene expression patterns. *Dev Dyn.* 2005;232:633-655.
2. Brock HW, Lohuizen MV. The Polycomb group-no longer an exclusive club? *Curr Opin Genet Dev.* 2001;11:175-181.
3. Sauvageau M, Sauvageau G. Polycomb group genes: keeping stem cell activity in balance. *PLoS Biol.* 2008;6(4):e113.
4. Classen AK, Bunker BD, Harvey KF, Vaccari T, Bilder D. A tumor suppressor activity of Drosophila Polycomb genes mediated by JAK-STAT signaling. *Nat Genet.* 2009;41(10):1150-1151.
5. Martinez AM, Schuettengruber B, Sakr S, Janic A, Gonzalez C, Cavalli G. Polyhomeotic has a tumor suppressor activity mediated by repression of Notch signaling. *Nat Genet.* 2009;41(10):1076-1082.
6. Fisher CL, Lee I, Bloyer S, et al. Additional sex combs-like 1 belongs to the enhancer of trithorax and polycomb group and genetically interacts with Cbx2 in mice. *Dev Biol.* 2010;337(1):9-15.
7. Fisher CL, Berger J, Randazzo F, Brock HW. A human homolog of Additional sex combs, ADDITIONAL SEX COMBS-LIKE 1, maps to chromosome 20q11. *Gene.* 2003;306:115-126.
8. Fisher CL, Randazzo F, Humphries RK, Brock HW. Characterization of Asxl1, a murine homolog of Additional sex combs, and analysis of the Asx-like gene family. *Gene.* 2006;369:109-118.
9. Kim K, Choi J, Heo K, et al. Isolation and characterization of a novel H1.2 complex that acts as a repressor of p53-mediated transcription. *J Biol Chem.* 2008;283(14):9113-9126.
10. Cho YS, Kim EJ, Park UH, Sin HS, Um SJ. Additional sex comb-like 1 (ASXL1), in cooperation with SRC-1, acts as a ligand-dependent coactivator for retinoic acid receptor. *J Biol Chem.* 2006; 281(26):17588-17598.
11. An Q, Wright SL, Konn ZJ, et al. Variable breakpoints target PAX5 in patients with dicentric chromosomes: a model for the basis of unbalanced translocations in cancer. *Proc Natl Acad Sci U S A.* 2008;105(44):17050-17054.
12. Gelsi-Boyer V, Trouplin V, Adelaide J, et al. Mutations of polycomb-associated gene ASXL1 in myelodysplastic syndromes and chronic myelomonocytic leukaemia. *Br J Haematol.* 2009; 145(6):788-800.
13. Baker LA, Allis CD, Wang GG. PHD fingers in human diseases: disorders arising from misinterpreting epigenetic marks. *Mutat Res.* 2008;647(1-2):3-12.
14. Chambers SP, Prior SE, Barstow DA, Minton NP. The pMTL nic- cloning vectors, I: improved pUC polylinker regions to facilitate the use of sonicated DNA for nucleotide sequencing. *Gene.* 1988;68(1):139-149.
15. Tybulewicz VLJ, Crawford CE, Jackson PK, Bronson RT, Mulligan RC. Neonatal lethality and lymphopenia in mice with a homozygous disruption of the *c-abl* proto-oncogene. *Cell.* 1991;65: 1153-1163.
16. Jacobs JJ, Keblusek P, Robanus-Maandag E, et al. Senescence bypass screen identifies TBX2, which represses Cdkn2a (p19(ARF)) and is amplified in a subset of human breast cancers. *Nat Genet.* 2000;26(3):291-299.
17. Pineault N, Helgason CD, Lawrence HJ, Humphries RK. Differential expression of Hox, Meis1, and Pbx1 genes in primitive cells throughout murine hematopoietic ontogeny. *Exp Hematol.* 2002;30(1):49-57.
18. Rodewald HR, Fehling HJ. Molecular and cellular events in early thymocyte development. *Adv Immunol.* 1998;69:1-112.
19. Tokimasa S, Ohta H, Sawada A, et al. Lack of the Polycomb-group gene rae28 causes maturation arrest at the early B-cell developmental stage. *Exp Hematol.* 2001;29(1):93-103.
20. Ohta H, Sawada A, Kim JY, et al. Polycomb group gene rae28 is required for sustaining activity of hematopoietic stem cells. *J Exp Med.* 2002; 195(6):759-770.
21. Nakorn TN, Miyamoto T, Weissman IL. Characterization of mouse clonogenic megakaryocyte progenitors. *Proc Natl Acad Sci U S A.* 2003; 100(1):205-210.
22. Calés C, Roman-Trufero M, Pavon L, et al. Inactivation of the polycomb group protein Ring1B unveils an antiproliferative role in hematopoietic cell expansion and cooperation with tumorigenesis associated with Ink4a deletion. *Mol Cell Biol.* 2008;28(3):1018-1028.
23. Coré N, Joly F, Boned A, Djabali M. Disruption of E2F signaling suppresses the INK4a-induced proliferative defect in M33-deficient mice. *Oncogene.* 2004;23(46):7660-7668.
24. Su IH, Basavaraj A, Krutchinsky AN, et al. Ezh2 controls B cell development through histone H3 methylation and Igh rearrangement. *Nat Immunol.* 2003;4(2):124-131.
25. Lessard J, Schumacher A, Thorsteinsdottir U, van Lohuizen M, Magnusson T, Sauvageau G. Functional antagonism of the *Polycomb*-Group genes *eed* and *Bmi1* in hemopoietic cell proliferation. *Genes Dev.* 1999;13:2691-2703.
26. Akasaka T, Tsuji K, Kawahira H, et al. The role of mel-18, a mammalian Polycomb group gene, during IL-7-dependent proliferation of lymphocyte precursors. *Immunity.* 1997;7(1):135-146.
27. van der Lugt MT, Domen J, Linders K, et al. Posterior transformation, neurological abnormalities, and severe hematopoietic defects in mice with a targeted deletion of the *bmi-1* proto-oncogene. *Genes Dev.* 1994;8:757-769.
28. Izon DJ, Rozenfeld S, Fong ST, Komuves L, Largman C, Lawrence HJ. Loss of function of the homeobox gene Hoxa-9 perturbs early T-cell development and induces apoptosis in primitive thymocytes. *Blood.* 1998;92(2):383-393.
29. Argiropoulos B, Humphries RK. Hox genes in hematopoiesis and leukemogenesis. *Oncogene.* 2007;26(47):6766-6776.
30. Lessard J, Schumacher A, Thorsteinsdottir U, van Lohuizen M, Magnuson T, Sauvageau G. Functional antagonism of the Polycomb-Group genes eed and Bmi1 in hemopoietic cell proliferation. *Genes Dev.* 1999;13(20):2691-2703.
31. Ohta H, Sawada A, Kim JY, et al. Polycomb group gene rae28 is required for sustaining activity of hematopoietic stem cells. *J Exp Med.* 2002; 195(6):759-770.
32. Ayton PM, Cleary ML. Transformation of myeloid progenitors by MLL oncoproteins is dependent on Hoxa7 and Hoxa9. *Genes Dev.* 2003;17(18): 2298-2307.
33. Yagi H, Deguchi K, Aono A, Tani Y, Kishimoto T, Komori T. Growth disturbance in fetal liver hematopoiesis of Mll-mutant mice. *Blood.* 1998;92(1): 108-117.
34. Madan V, Madan B, Brykczynska U, et al. Impaired function of primitive hematopoietic cells in

mice lacking the Mixed-Lineage-Leukemia homolog MLL5. *Blood.* 2009;113(7):1444-1454.

35. Heuser M, Yap DB, Leung M, et al. Loss of MLL5 results in pleiotropic hematopoietic defects, reduced neutrophil immune function, and extreme sensitivity to DNA demethylation. *Blood.* 2009; 113(7):1432-1443.
36. Zhang Y, Wong J, Klinger M, Tran MT, Shannon KM, Killeen N. MLL5 contributes to hematopoietic stem cell fitness and homeostasis. *Blood.* 2009; 113(7):1455-1463.
37. Majewski IJ, Blewitt ME, de Graaf CA, et al. Polycomb repressive complex 2 (PRC2) restricts hematopoietic stem cell activity. *PLoS Biol.* 2008; 6(4):e93.
38. Arai S, Miyazaki T. Impaired maturation of myeloid progenitors in mice lacking novel Polycomb group protein MBT-1. *EMBO J.* 2005;24(10): 1863-1873.
39. Katoh-Fukui Y, Tsuchiya R, Shiroishi T, et al. Male-to-female sex reversal in *M33* mutant mice. *Nature.* 1998;393:688-692.
40. Coré N, Bel S, Gaunt SJ, et al. Altered cellular proliferation and mesoderm patterning in Polycomb-M33-deficient mice. *Development.* 1997;124:721-729.
41. Akasaka T, Kanno M, Balling R, Mieza MA, Taniguchi M, Koseki H. A role for *mel-18*, a Polycomb group related vertebrate gene, during the anteroposterior specification of the axial skeleton. *Development.* 1996;122:1513-1522.
42. Ernst P, Fisher JK, Avery W, Wade S, Foy D, Korsmeyer SJ. Definitive hematopoiesis requires the mixed-lineage leukemia gene. *Dev Cell.* 2004;6(3):437-443.
43. Lessard J, Sauvageau G. Bmi-1 determines the proliferative capacity of normal and leukaemic stem cells. *Nature.* 2003;423(6937):255-260.
44. Park IK, Qian D, Kiel M, et al. Bmi-1 is required for maintenance of adult self-renewing haematopoietic stem cells. *Nature.* 2003;423(6937):302-305.
45. Kim JY, Sawada A, Tokimasa S, et al. Defective long-term repopulating ability in hematopoietic stem cells lacking the Polycomb-group gene rae28. *Eur J Haematol.* 2004;73(2):75-84.
46. National Center for Biotechnology Information. GenBank. http://www.ncbi.nlm.nih.gov/Genbank. Accessed April 25, 2002.
47. Katoh M. Identification and characterization of ASXL2 gene in silico. *Int J Oncol.* 2003;23(3): 845-850.
48. Scotto L, Narayan G, Nandula SV, et al. Identification of copy number gain and overexpressed genes on chromosome arm 20q by an integrative genomic approach in cervical cancer: potential role in progression. *Genes Chromosomes Cancer.* 2008;47(9):755-765.
49. Mackinnon RN, Campbell LJ. Dicentric chromosomes and 20q11.2 amplification in MDS/AML with apparent monosomy 20. *Cytogenet Genome Res.* 2007;119(3-4):211-220.
50. Wilting SM, Snijders PJ, Meijer GA, et al. Increased gene copy numbers at chromosome 20q are frequent in both squamous cell carcinomas and adenocarcinomas of the cervix. *J Pathol.* 2006;209(2):220-230.
51. Tonon G, Wong KK, Maulik G, et al. High-resolution genomic profiles of human lung cancer. *Proc Natl Acad Sci U S A.* 2005;102(27):9625-9630.
52. Sun SY, Lotan R. Retinoids and their receptors in cancer development and chemoprevention. *Crit Rev Oncol Hematol.* 2002;41(1):41-55.

Pediatr Transplantation 2009

© 2009 John Wiley & Sons A/S.

Pediatric Transplantation
DOI: 10.1111/j.1399-3046.2009.01217.x

Hemophagocytosis after bone marrow transplantation for JAK3-deficient severe combined immunodeficiency

Hashii Y, Yoshida H, Kuroda S, Kusuki S, Sato E, Tokimasa S, Ohta H, Matsubara Y, Kinoshita S, Nakagawa N, Imai K, Nonoyama S, Oshima K, Ohara O, Ozono K. Hemophagocytosis after bone marrow transplantation for JAK3-deficient severe combined immunodeficiency. Pediatr Transplantation 2009. © 2009 John Wiley & Sons A/S.

Abstract: HSCT is the optimal treatment for patients with SCID. In particular, HSCT from a HLA-identical donor gives rise to successful engraftment with long survival. We report a six-month-old girl with JAK3-deficient SCID who developed hemophagocytosis after BMT without conditioning from her HLA-identical father. She had suffered from pneumonia and hepatitis before BMT. Prophylaxis for GVHD was short-term methotrexate and tacrolimus. On day 18 after BMT, the patient developed hemophagocytosis in bone marrow when donor lymphocytes were increasing in peripheral blood. Analysis of chimerism confirmed host origin of macrophages and donor origin of lymphocytes. Thus, host macrophage activation was presumably induced in response to donor lymphocytes through immunoreaction to infections and/or alloantigens. HSCT for SCID necessitates caution with respect to hemophagocytosis.

Yoshiko Hashii[1], Hisao Yoshida[1], Sato Kuroda[1], Shigenori Kusuki[1], Emiko Sato[1], Sadao Tokimasa[1], Hideaki Ohta[1], Yasutaka Matsubara[2], Seiji Kinoshita[2], Noriko Nakagawa[3], Kohsuke Imai[3], Shigeaki Nonoyama[3], Koichi Oshima[4,5], Osamu Ohara[4,5] and Keiichi Ozono[1]

[1]Department of Pediatrics, Osaka University Graduate School of Medicine, Suita, Japan, [2]Department of Pediatrics, Higashiosaka City General Hospital, Higashiosaka, Japan, [3]Department of Pediatrics, National Defense Medical College, Tokorozawa, Japan, [4]Department of Human Genome Technology, Kazusa DNA Research Institute, Kisarazu, Japan, [5]Laboratory for Immunogenomics, Research Center for Allergy and Immunology, RIKEN Yokohama Institute, Yokohama, Japan

Key words: bone marrow transplantation – hemophagocytosis – JAK3 mutation – severe combined immunodeficiency

Yoshiko Hashii, Department of Pediatrics, Osaka University Graduate School of Medicine, 2-2 Yamadaoka, Suita, Osaka 565-0871, Japan
Tel.: +81-6-6879-3932
Fax: +81-6-6879-3939
E-mail: yhashii@ped.med.osaka-u.ac.jp

Accepted for publication 3 June 2009

SCID is a uniformly fatal disease unless promptly treated with HSCT, which reconstitutes a normal immune system (1–3). Patients with SCID have often been affected by various kinds of infections prior to HSCT and the presence of pulmonary infection is a powerful predictor of death after HSCT (1). In addition, hemophagocytosis has been reported as an important complication early after HSCT (4–7). This phenomenon is in many cases triggered by infections (4, 5) and in some cases by an alloimmune response (6, 7). We report a girl with JAK3-deficient SCID who developed hemophagocytosis after BMT without conditioning from her HLA-identical father, where donor lymphocytes presumably activated host macrophages.

Abbreviations: γc, γ chain; BCG, Bacille de Calmette et Guérin; BM, bone marrow; BMT, bone marrow transplantation; CMV, cytomegalovirus; EBV, Epstein-Barr virus; FISH, fluorescence *in situ* hybridization; GVHD, graft-versus-host disease; HHV, human herpes virus; HLA, human leukocyte antigen; HSCT, hematopoietic stem cell transplantation; HSV, herpes simplex virus; IFN, interferon; IL, interleukin; m-PSL, methyl PSL; NK, natural killer; PCR, polymerase chain reaction; PSL, prednisolone; RT, reverse transcription; SCID, severe combined immunodeficiency; TNF, tumor necrosis factor; TRECs, T-cell-receptor excision circles; VNTR, variable number of tandem repeat.

Case report

A five-month-old girl, born to consanguineous Chinese parents, had repeatedly developed viral and bacterial bronchitis and oral candidiasis

from two months of age. She had received no BCG vaccination. White blood cell count was 2690/μL (63.5% neutrophils, 27.1% lymphocytes, 1.6% eosinophils, 0% basophils, 7.8% monocytes). Serum IgG, IgA, and IgM levels were 213, 1, and 34 mg/dL, respectively. Lymphocyte subset analysis showed absence of T lymphocytes (0.6% $CD3^+$, 0.3% $CD4^+$, 1.2% $CD8^+$) and NK cells (1.6% $CD16^+$, 0.6% $CD56^+$) with normal numbers of B lymphocytes (96.9% $CD19^+$, 97.3% $CD20^+$). A diagnosis of $T^-B^+NK^-$SCID was made, and genetic analysis revealed a novel homozygous non-sense mutation of JAK3: a C to T point mutation at nucleotide 623 that changed amino acid 175 in the JH6 domain from arginine to a stop codon (C623T; R175X) (Fig. 1).

The clinical course of the patient is summarized in Fig. 2. When she was referred to our hospital, she suffered from severe interstitial pneumonia and liver dysfunction. No sign of infection was observed on studies by RT-PCR of her serum for CMV, HHV6, HHV7, adenovirus, HSV-1 or -2, and EBV genomes. *Aspergillus* spp. and *Pneumocystis jiroveci* were not detected in her sputa by PCR analysis. β-D-glucan was not detected in her serum. She received oxygen therapy and infusion of hyperalimentation because of poor feeding.

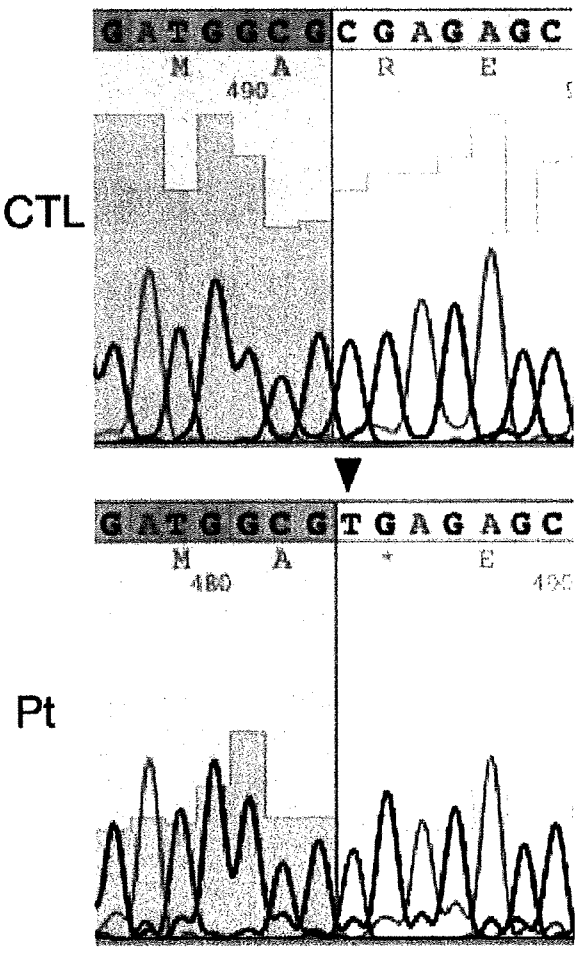

Fig. 1. Sequence analysis showing a non-sense mutation. The JAK3 gene of the patient showed a C to T point mutation (C623T) as shown by arrowhead. CTL, control; Pt, patient.

At the age of six months, she underwent unmanipulated BMT from her genotypically HLA-identical father without conditioning. Both the patient and her father had the same HLA genotype: HLA-A*0101/3001-B*1302/3701-C*0602-DRB1*0701/1501.

Prophylaxis for GVHD was short-term methotrexate (days 1, 3, 6, and 11) and tacrolimus. She developed grade 3 acute GVHD with watery diarrhea (stage 2) and skin eruption (stage 1) on day 9 after BMT, for which she was treated with 2 mg/kg/day of PSL. On day 16, her interstitial pneumonia deteriorated in both lungs on chest X-ray. RT-PCR analysis of sputa showed negative results of CMV, *Aspergillus* spp., and *P. jiroveci.*

Her WBC count decreased to 330/μL on day 18 and BM aspiration revealed hypoplastic marrow with hemophagocytosis by activated macrophages (nuclear cell count, 4000/μL; megakaryocyte count, 0/μL) (Fig. 3). Serum ferritin level was 715 ng/mL and serum soluble IL-2 receptor level was 3295 U/mL. Hemophagocytosis improved three days after administration of etoposide 30 mg/m^2 and pulsed m-PSL 30 mg/kg/day on day 18. VNTR analysis revealed that donor cells were almost completely absent from whole cells and macrophages ($CD14^+$ cells) of the BM cells on days 18 and 20, respectively (Fig. 4). Meanwhile, donor cells were detected in peripheral blood cells on days 20 and 24, including T lymphocytes ($CD3^+$ cells) on day 24 (Fig. 4). A serial flow cytometric analysis of lymphocyte-gated cells also demonstrated that $CD3^+$ cells with predominance of $CD4^+$ cells, most likely donor cells, increased to 3.59% and 5.03% on days 18 and 21, respectively (Table 1). Furthermore, FISH analysis of sex chromosome detected donor cells in 10.8% and 8.6% of peripheral blood cells on days 20 and 28, respectively (data not shown).

As her respiratory condition deteriorated, she received repeated courses of pulsed m-PSL (30 mg/kg/day) therapy and underwent mechanical ventilation on day 20. Despite intensive therapy, she died on day 32 due to respiratory failure. Lung necropsy showed necrotized cells

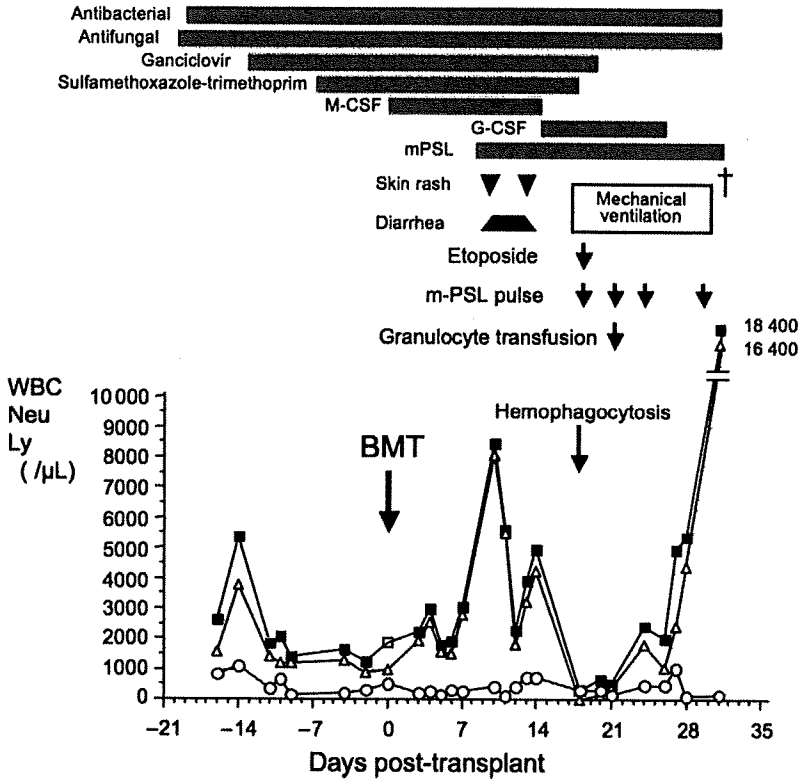

Fig. 2. Clinical course and changes in white blood cell counts. WBC, white blood cells (solid squares); Neu, neutrophil (open triangles); Ly, lymphocyte (open circles); M-CSF, macrophage-colony stimulating factor; G-CSF, granulocyte-colony stimulating factor.

without inflammatory cells. No bacterial, viral, or fungal components were detected in the tissue.

Discussion

SCID is a rare syndrome with heterogeneous genetic inheritance. Common γc mutations have been identified in X-linked SCID, characterized by lack of T cells and NK cells with presence of B cells ($T^-B^+NK^-$SCID). JAK3 mutations have been identified in some patients of autosomal SCID, which shares similar clinical features to X-linked SCID but with normal γc (8–10). JAK3,

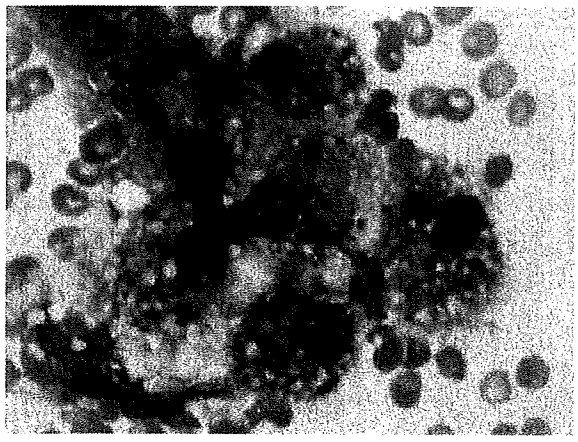

Fig. 3. Bone marrow aspiration on day 18 showing aggregate of activated macrophages. On the far right an erythroblast appears to be undergoing endocytosis.

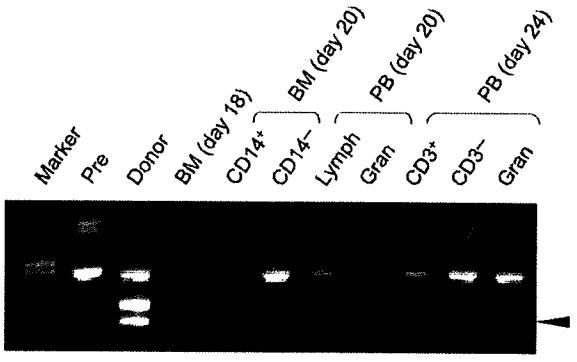

Fig. 4. VNTR analysis. Specific primers designed to flank the repetitive unit, D1S80, were used for the PCR (17). Amplified DNA was electrophoresed and visualized with ethidium bromide. $CD14^+$ or $CD3^+$ cells were purified by magnetic cells sorting enrichment kit (MACS: Miltenyi Biotec GmbH, Bergisch Gladbach, Germany). Arrowhead indicates a donor-specific band. Prespecific bands cannot be separated from donor-specific bands.

Table 1. Flow cytometric analysis of lymphocyte-gated cells in peripheral blood

	Lymphocytes (μL)	CD19 (%)	CD3 (%)	CD4 (%)	CD8 (%)	CD56 (%)
Pre (Day −15)	838	96.7	0.55	NE	NE	1.46
Day +7	243	87.9	2.82	1.31	0.44	0.28
Day +11	111	98.4	0.53	NE	NE	0.34
Day +13	707	98.6	0.39	NE	NE	0.15
Day +18	330	91.6	3.59	3.28	ND	0.24
Day +21	167	88.3	5.03	4.15	0.52	0.88

NE, not evaluable; ND, not done.

a member of the Janus family intracellular protein kinases, associates with intracellular domain of γc and is required for signal transduction from γc-containing receptors (8–10). To date, more than 30 mutations of JAK3 have been reported according to RAPID (Resource of Asian Primary Immunodeficiency Database) (http://rapid.rcai.riken.jp/RAPID/mutation?pid_id=AGID_86); most of them are sporadic and lacking preferential hot spots.

The JAK3 gene has an open reading frame of 3372 bp that is translated into a 1124 amino acid protein (10). In our patient, we identified a novel non-sense homozygous mutation (C623T; Arg157X) leading to a premature stop codon in the JH6 domain. Although we did not evaluate protein expression, this non-sense mutation, nearer to the amino-terminus, probably resulted in abrogated protein expression. The homozygosity was in line with other reported cases with parental consanguinity (8).

Prompt HSCT is an effective life-saving treatment modality for reconstitution of T-cell immunity in this defect (1–3). Our patient therefore underwent BMT immediately after diagnosis from her genotypically HLA-identical father without conditioning. A large European study (1), which analyzed 475 HSCTs for SCID from 1968 to 1999, showed 81% and 72% three-yr survival after HSCT in patients after HSCT from genotypically and phenotypically HLA-identical related donors, respectively. This study furthermore reported 96% sustained engraftment from HLA-identical HSCT, and better engraftment at 93% in SCID with B-cell-positive phenotype, i.e., γc- or JAK3-deficient SCID, compared with 88% in SCID with B-cell-negative phenotype. Recent studies also showed successful HSCT outcome with >90% survival with engraftment in SCID including γc- or JAK3-deficient SCID (2, 3).

Hemophagocytosis early after HSCT has been reported as an important complication (4–7), which is thought to be caused by infections (4, 5) or an alloimmune response (6, 7). The previous reports did not show any detailed analysis of macrophage origin, and the exact mechanism of macrophage activation remains unclear. Moreover, hemophagocytosis after HSCT for SCID as the cause of the graft failure has been reported in only some cases. Norris et al. (11) reported hemophagocytosis after three months HSCT in a T^-B^+ SCID patient who had received T cell-depleted HSCT from an HLA-haploidentical donor without a conditioning regimen. They demonstrated that the hemophagocytosis occurred as a result of donor T-cell engraftment with incomplete immune function, since B-cell reconstitution and tri-lineage hematopoiesis including macrophages showed host type. In our case, hemophagocytosis also occurred after donor T-cell engraftment.

Our patient developed hemophagocytosis and respiratory distress, accompanied by unexpected slow and low engraftment of donor cells. Hemophagocytosis was caused by host macrophages when donor lymphocytes were increasing. Since the patient congenitally had no functioning T cells, it is most probable that donor lymphocytes responded to host cells or resident infectious organisms, leading to IFN-γ production and to activation of host macrophages (12, 13). In SCID patients, maternal engraftment of T cells can lead to GVHD of the skin and liver. Dvorak et al. (14) reported that the T(-)B(+) NK(-) SCID patient with complete CD132 deficiency represented hemophagocytosis without GVHD and that hemophagocytosis was most likely caused by maternal perforin-expressing CD8 T cells. In our case, maternal T cells were not detected pre-SCT (Table 1), which suggests that paternal CD8 T cells or NK cells were involved in hemophagocytosis.

Monocyte function in JAK3-deficient SCID patients has been reported to be intact with respect to cytokine production in response to stimulation (15). The activated macrophages, in turn, probably produced the pro-inflammatory cytokines, TNFα, IL-1β, and IL-6 (12, 13), which might have caused the lung injury as no organism was detected by post-mortem examination.

A conditioning regimen is generally not administered to SCID patients during HSCT from HLA-identical related donors (1–3). However, in our patient, residual macrophages would appear to play an important role in causing hemophagocytosis, which might have led to poor engraftment. Furthermore, Cavazzana et al. (16) analyzed primary T-cell-immunodeficient patients who had undergone HSCT and demonstrated that all patients having undergone full myeloablation had donor myeloid cells and persistent

thymopoiesis, as evidenced by the presence of naive T cells carrying TRECs, which indicates the importance of the complete absence of thymic progenitors by myeloablative conditioning in providing a favorable environment for thymic seeding by early progenitor cells. Our results lead us to surmise that, even when transplanted from an HLA-identical donor, some kind of immunosuppressive conditioning is needed to prevent hemophagocytosis.

In conclusion, we describe a child with JAK3-deficient SCID who developed hemophagocytosis after HSCT from her HLA-identical father. Host macrophage activation would appear to be induced by donor lymphocytes through immune reaction to alloantigen or infectious organisms. HSCT for SCID necessitates caution with respect to hemophagocytosis.

Acknowledgment

We thank Ms. Tokuko Okuda for performing the flow cytometric analysis and VNTR analysis.

References

1. Antoine C, Muller S, Cant A, et al. Long-term survival and transplantation of haemopoietic stem cells for immunodeficiencies: Report of the European experience 1968–99. Lancet 2003: 361: 553–560.
2. Roberts JL, Lengi A, Brown SM, et al. Janus kinase 3 (JAK3) deficiency: Clinical, immunologic, and molecular analyses of 10 patients and outcomes of stem cell transplantation. Blood 2004: 103: 2009–2018.
3. Grunebaum E, Mazzolari E, Porta F, et al. Bone marrow transplantation for severe combined immune deficiency. JAMA 2006: 295: 508–518.
4. Levy J, Wodell RA, August CS, Bayever E. Adenovirus-related hemophagocytic syndrome after bone marrow transplantation. Bone Marrow Transplant 1990: 6: 349–352.
5. Sato M, Matsushima T, Takada S, et al. Fulminant, CMV-associated, haemophagocytic syndrome following unrelated bone marrow transplantation. Bone Marrow Transplant 1998: 22: 1219–1222.
6. Ishikawa J, Maeda T, Miyazaki T, et al. Early onset of hemophagocytic syndrome following allogeneic bone marrow transplantation. Int J Hematol 2000: 72: 243–246.
7. Abe Y, Choi I, Hara K, et al. Hemophagocytic syndrome: A rare complication of allogeneic nonmyeloablative hematopoietic stem cell transplantation. Bone Marrow Transplant 2002: 29: 799–801.
8. Notarangelo LD, Mella P, Jones A, et al. Mutations in severe combined immune deficiency (SCID) due to JAK3 deficiency. Hum Mutat 2001: 18: 255–263.
9. O'shea JJ, Husa M, Li D, et al. Jak3 and the pathogenesis of severe combined immunodeficiency. Mol Immunol 2004: 41: 727–737.
10. Pesu M, Candotti F, Husa M, Hofmann SR, Notarangelo LD, O'shea JJ. Jak3, severe combined immunodeficiency, and a new class of immunosuppressive drugs. Immunol Rev 2005: 203: 127–142.
11. Norris R, Paessler M, Bunin N. Donor T-cell-mediated pancytopenia after haploidentical hematopoietic stem cell transplant for severe combined immunodeficiency. J Pediatr Hematol Oncol 2009: 31: 148–150.
12. Larroche C, Mouthon L. Pathogenesis of hemophagocytic syndrome (HPS). Autoimmun Rev 2004: 3: 69–75.
13. Rouphael NG, Talati NJ, Vaughan C, Cunningham K, Moreira R, Gould C. Infections associated with haemophagocytic syndrome. Lancet Infect Dis 2007: 7: 814–822.
14. Dvork CC, Sandford A, Fong A, et al. Maternal T-cell engraftment associated with severe hemophagocytosis of the bone marrow in untreated X-linked severe combined immunodeficiency. J Pediatr Hematol Oncol 2008: 30: 396–400.
15. Villa A, Sironi M, Macchi P, et al. Monocyte function in a severe combined immunodeficient patient with a donor splice site mutation in the Jak3 gene. Blood 1996: 88: 817–823.
16. Cavazzana-Calvo M, Carlier F, Le Deist F, et al. Long-term T-cell reconstitution after hematopoietic stem-cell transplantation in primary T-cell-immunodeficient patients is associated with myeloid chimerism and possibly the primary disease phenotype. Blood 2007: 109: 4575–4581.
17. Budowle B, Chakraborty R, Giusti AM, Eisenberg AJ, Allen RC. Analysis of the VNTR locus D1S80 by the PCR followed by high-resolution PAGE. Am J Hum Genet 1991: 48: 137–144.

Molecular Genetics and Metabolism 98 (2009) 255–263

Contents lists available at ScienceDirect

Molecular Genetics and Metabolism

journal homepage: www.elsevier.com/locate/ymgme

Localized donor cells in brain of a Hunter disease patient after cord blood stem cell transplantation

Ken Araya [a], Norio Sakai [a], Ikuko Mohri [a,b], Kuriko Kagitani-Shimono [a], Takeshi Okinaga [a], Yoshiko Hashii [a], Hideaki Ohta [a], Itsuko Nakamichi [c], Katsuyuki Aozasa [c], Masako Taniike [a,b,*], Keiichi Ozono [a]

[a] Department of Pediatrics, Osaka University Graduate School of Medicine, 2-2 Yamadaoka, Suita, Osaka 565-0871, Japan
[b] Department of Molecular Research Center for Children's Mental Development, Osaka University Graduate School of Medicine, 2-2 Yamadaoka, Suita, Osaka 565-0871, Japan
[c] Department of Histopathology, Osaka University Graduate School of Medicine, 2-2 Yamadaoka, Suita, Osaka 565-0871, Japan

ARTICLE INFO

Article history:
Received 21 May 2009
Accepted 21 May 2009
Available online 24 May 2009

Keywords:
Neuropathology
Immunohistochemistry
Hunter disease
Mucopolysaccharidosis II
Cord blood stem cell transplantation
Iduronate-2-sulfatase

ABSTRACT

The efficacy of hematopoietic stem cell transplantation (HSCT) for Hunter disease (deficiency of iduronate-2-sulfatase, IDS) remains unclear. We treated a 6-year-old male suffering from a severe type of Hunter disease with cord blood stem cell transplantation (CBSCT); however, he died at 10 months post-therapy due to a laryngeal post-transplantation lymphoproliferative disorder. During the follow-up period after CBSCT, his hyperactivity, estimated mental age, and brain MR findings had not improved. We assessed the efficacy of CBSCT by biochemical and pathological analyses of the autopsied tissues. There were many distended cells with accumulated substrate in the brain, but not in the liver. IDS enzyme activity in the cerebrum remained very low, although that in the liver reached about 40% of the normal control level. However, a variable number of tandem repeats analyses demonstrated a weak donor-derived band not only in the liver but also in the cerebrum. Furthermore, IDS-immunoreactivity in the liver was recognized broadly not only in Kupffer cells but also in hepatocytes. On the other hand, IDS-immunoreactivity was recognized exclusively in CD68-positive microglia/monocytes in the patient's brain; whereas that in the normal brain was also detected in neurons and oligodendrocytes. These donor-derived IDS-positive cells were predominantly localized in perivascular spaces and some of them were evidently present in the brain parenchyma. The efficacy of CBSCT was judged to be insufficient for the brain at 10 months post-therapy. However, the pathological detection of donor-derived cells in the brain parenchyma suggests the potential of HSCT for treatment of neurological symptoms in Hunter disease. This is the first neuropathological report documenting the distribution of donor-derived cells in the brain after CBSCT into a Hunter disease patient.

© 2009 Elsevier Inc. All rights reserved.

1. Introduction

Hunter disease [1], mucopolysaccharidosis (MPS) II (MIM +309900), is an X-linked recessive lysosomal storage disorder (LSD) that arises due to a deficiency of iduronate-2-sulfatase (IDS: EC 3.1.6.13), and leads to the accumulation of glycosaminoglycan (GAG) in various organs including the central nervous system (CNS). In the CNS, distended cells with large clear vacuoles are observed, and dilatation of the perivascular (Virchow–Robin) space is conspicuous within the cerebral white matter. The neuronal storage materials are positive by periodic acid Schiff (PAS) staining [2]. A considerable degree of neuronal loss and gliosis is common [3]. The accumulated substrate with membranous cytoplasmic bodies or Zebra bodies is observed in electron micrographs [4,5]. In the liver, hepatocytes and Kupffer cells are also swollen with a vacuolated cytoplasm, and accumulated substrate in them is positive by colloidal iron staining [6,7].

The patients present with multiple progressive symptoms such as coarse facial features, skeletal deformities, hepatosplenomegaly, respiratory tract infection, cardiovascular disorders, and various degrees of CNS involvement. There is a wide spectrum from mild to severe types, which are classified on clinical grounds because IDS activity appears equally deficient in both types. Although the mild type is characterized by preservation of intelligence, the severe type, with onset usually occurring between 2 and 4 years of age, is characterized by mental retardation and death before adulthood mainly due to obstructive airway disease and cardiac failure [8].

There have been no established treatments for MPS II; however, 2 therapeutic possibilities have been pursued, that is, hematopoietic stem cell transplantation (HSCT) and enzyme replacement therapy (ERT). Although the enzyme administered intravenously by ERT is not expected to cross the blood–brain barrier (BBB) [9],

* Corresponding author. Address: Department of Pediatrics, Osaka University Graduate School of Medicine, 2-2 Yamadaoka, Suita, Osaka 565-0871, Japan.
E-mail address: masako@ped.med.osaka-u.ac.jp (M. Taniike).

1096-7192/$ - see front matter © 2009 Elsevier Inc. All rights reserved.
doi:10.1016/j.ymgme.2009.05.006

HSCT is considered to provide a constant source of enzyme replacement through the engrafted donor cells, which are not impeded by the BBB and can thus deliver the enzyme to the CNS [10]. Several *in vitro* studies using cultured cells [11] and *in vivo* ones using model animals [12–14] have confirmed the biochemical, pathological or functional improvement; therefore, many LSD patients have been treated with HSCT over the last 25 years [15]. However, only a few studies have reported about the pathological evaluation of the human CNS after HSCT [16,17].

Here we document a clinicopathological evaluation of the efficacy of umbilical cord blood stem cell transplantation (CBSCT) on the neuropathology made by detecting the accumulated substrate and donor-derived cells in the autopsied tissue of a 6-year-old male with a severe type of MPS II, involving moderate mental retardation and brain atrophy, 10 months after CBSCT. Since sex-matched transplantation had been performed, the strategy of the detection of donor cells by the use of fluorescence *in situ* hybridization for sex chromosomes [18] was not available. Therefore, the detection of donor cells was performed by immunohistochemical demonstration of IDS-positive cells, assays of IDS activity, and variable number of tandem repeats (VNTR) analysis.

2. Patient, materials, and methods

2.1. Patient and case history

The patient was born by normal delivery at 40 weeks' gestation. His developmental milestones were normal by the age of 18 months; however, a delay in his language and motor skills was first recognized at the age of 2 years. He was suspected of suffering from MPS II because of the developmental delay, the characteristic facial features, and the characteristic X-ray findings of skeletal deformities. At the age of 3 years 8 months, the diagnosis of MPS II was confirmed based on the low activity of IDS in his lymphocytes (0.5 nmol/4 h/mg vs. adult control range of 58.4–114 nmol/4 h/mg, measured by SRL Inc., Tokyo, Japan). Genetic analysis revealed that he harbored a nonsense mutation, W267X, in exon 6 of his IDS gene on Xq28.1.

At the age of 5 years 11 months, CBSCT was performed by using cells from an unrelated male donor who had completely matched HLA phenotypes but 3 loci mismatched HLA genotypes (donor/recipient: A0201/0206, DR0406/0410, DR1406/1402), after obtaining informed consent from his parents. The conditioning regimen for CBSCT consisted of busulfan, cyclophosphamide, and fludarabine. He received short-term methotrexate (15 mg/m^2 on day 1, 10 mg/m^2 on days 3, 6, and 11) and tacrolimus of which whole blood concentration was maintained at a trough level of 5–15 ng/ml. The detailed protocol was described by Tokimasa et al. (as Patient 5) [19]. He had not experienced chronic graft-versus-host-disease (GVHD) but only grade I acute GVHD requiring no steroid therapy. His bone marrow was confirmed to be completely of the donor type by VNTR analysis 1 month, 6 months, and 9 months after CBSCT (Supplemental Fig. 1). However, at the age of 6 years 7 months, he developed severe upper-airway obstruction necessitating intensive care. The biopsy of his swollen larynx yielded the diagnosis of Epstein–Barr virus-unassociated post-transplantation lymphoproliferative disorder, and his condition deteriorated despite 6 courses of rituximab administration. He eventually died at the age of 6 years 9 months, that is, 10 months post-CBSCT.

At the age of 5 years 11 months, just before CBSCT, he was hyperactive and had an estimated mental age of 28 months. His liver was palpable 6 cm below the right costal margin. By the age of 6 years 6 months, 7 months post-CBSCT, his hyperactivity and mental retardation had not changed significantly (estimated mental age of 30 months), although his hepatomegaly had improved (palpable 3 cm below the right costal margin).

2.2. Materials and post-mortem brain tissue processing

We performed a general autopsy of the patient after having obtained written informed consent from his parents. The post-mortem interval (PMI) was 3 h. At the autopsy, small blocks of liver and brain samples were snap-frozen or fixed for the electron microscopical investigation. After 10 months of formalin-fixation, blocks from cerebrum, hippocampus, and cerebellum were cut out and used for the study. For comparative analysis, formalin-fixed brain blocks (13 months of fixation) from a 6-year-5-month-old boy who had died in our hospital were used as a non-MPS II control, with informed consent. The formalin-fixed brain blocks were embedded in *Tissue-Tek* Optimal Cutting Temperature compound (Sakura Finetek Inc., Torrance, CA, USA) after immersion for 6 days in 0.1 M phosphate buffer (PB) in which the concentration of saccharose was increased from 5% to 30%, by 5% per day. Thereafter, they were quickly frozen and sectioned at 5 μm by a cryostat (*JUNG CM* 1800, Leica Microsystems GmbH, Wetzlar, Germany) and mounted onto the aminosilane-coated microscope slides (Matsunami Glass Ind. Ltd., Osaka, Japan).

In addition, we obtained unfixed-frozen cerebrum samples from an 11-year-old untreated MPS II patient and a 12-year-old non-MPS II control, whose PMI were 15 h and 18.5 h, respectively, from the NICHD Brain and Tissue Bank for Developmental Disorders at the University of Maryland, Baltimore, MD, USA. The unfixed-frozen cerebral samples were sectioned at 5 μm, mounted onto aminosilane-coated microscope slides, and fixed by immersion in 20% formaldehyde solution for 5 min at room temperature. Furthermore, we obtained three unfixed-frozen liver samples from non-MPS II controls (2–7 years old) from Dr. Masahiro Nakayama, Osaka Medical Center and Research Institute for Maternal and Child Health, Osaka, Japan.

This study was approved by the Institutional Review Boards of Osaka University Graduate School of Medicine.

2.3. Methods

2.3.1. Colloidal iron staining study

After having been rinsed in 12% acetic acid, 5 μm-thick unfixed-frozen liver sections were placed in a solution of 0.25% ferric chloride and 12% acetic acid for 1 h. They were then rinsed again in 12% acetic acid, immersed in a mixture of 2.5% potassium ferrocyanide and 2.5% hydrochloric acid, and counterstained with 0.1% nuclear fast red and 5% aluminum sulfate. They were observed under a Microscope BX40 (Olympus Co., Tokyo, Japan) equipped with a high-sensitivity cooled CCD color camera VB-7010 (Keyence Co., Osaka, Japan).

2.3.2 PAS staining studies

The brain sections were oxidized with 0.5% orthoperiodic acid, and placed in Lillie's Cold Schiff's Reagent (0.5% basic fuchsin, 100 mM hydrochloric acid, and 0.5% acid sodium sulfite). They were then rinsed in 0.5% sodium bisulfite and 50 mM hydrochloric acid, counterstained with Mayer's hematoxylin (Wako Pure Chemical Industries Ltd., Osaka, Japan), and observed under the Microscope BX40.

2.3.3. Electron microscope (EM) studies

The cerebral and cerebellar samples were fixed with 1% paraformaldehyde and 3% glutaraldehyde in 0.1 M PB, postfixed in 1% osmium tetroxide, stained with 1% uranyl acetate, and embedded in *Epon* 812 (TAAB Laboratories Equipment Ltd., Berkshire, UK). After

observation of semi-thin sections, ultra-thin sections were stained with lead citrate and observed under a Transmission Electron Microscope H-7650 (Hitachi High-Technologies Co., Tokyo, Japan).

2.3.4. Enzyme assays

Each unfixed tissue sample was homogenized mechanically in ice-cold deionized water. After having been frozen and thawed, the homogenate was centrifuged at 1000*g* for 10 min. After the determination of protein concentration by the Lowry method [20], each supernatant was used for enzyme assays. The enzyme activity of IDS was measured by the method described by Voznyi et al. [21], and those activities of β-galactosidase (EC 3.2.1.23) and β-hexosaminidase (EC 3.2.1.52) were measured as described by Hindman and Cotlier [22].

2.3.5. VNTR analysis

Deoxyribonucleic acid (DNA) samples (0.2 μg), extracted from each blood or tissue sample, were amplified with 35 cycles of polymerase chain reaction in a reaction mixture containing 50 μl of 200 μM deoxynucleotide triphosphate mixture, 2.5 U of *AmpliTaq Gold* DNA Polymerase (Applied Biosystems Inc., Foster City, CA, USA), 10 mM Tris–hydrochloric acid (pH 8.3), 50 mM potassium chloride, 1.5 mM magnesium chloride, and an 1 μM concentration of each primer for amplification of a polymorphic DNA sequence (pMCT118) on chromosome 1p (D1S80) [23,24]. Each cycle consisted of 1 min at 95 °C for denaturation, 1 min at 65 °C for annealing, and 2 min at 70 °C for extension. After amplification, polymorphic bands were detected by agarose gel electrophoresis.

2.3.6. Immunoblot analysis

After solubilization in lysis buffer (50 mM Tris, 150 mM NaCl, 1 mM EDTA, 1% NP-40, 0.25% Na-deoxycholate, 2 μg/ml aprotinin, 2 μg/ml leupeptin, 2 μg/ml pepstatin A, 0.5 mM phenylmethylsulfonyl fluoride, and 1 mM dithiothreitol), 40 ng and 0.4 ng recombinant human IDS (*Elaprase*, Shire Human Genetic Therapies Inc., Cambridge, MA, USA) and 40 ng recombinant human α-glucosidase (*Myozyme*, Genzyme Co., Cambridge, MA, USA) as a negative control were separated by sodium dodecyl sulfate–polyacrylamide gel electrophoresis and transferred electrophoretically to a nitrocellulose membrane (*Trans-Blot* Transfer Medium, Bio-Rad Laboratories Inc., Hercules, CA, USA). The membrane was incubated overnight at 4 °C with goat antibody against IDS (0.1 μg/ml, AF2449, R&D Systems Inc., Minneapolis, MN, USA) after treatment with 5% skim milk/Tris-buffered saline for blocking nonspecific reactions. The immune complexes were detected with peroxidase-labeled horse anti-goat IgG (1:10,000, Vector Laboratories Inc., Burlingame, CA, USA) and *SuperSignal* West Dura Extended Duration Substrate (Pierce Chemical Co., Rockford, IL, USA).

2.3.7. Immunohistochemical studies

Brain sections were incubated for 30 min in 0.3% hydrogen peroxide/methanol for quenching endogenous peroxidase activity, and then pretreated with 1% bovine serum albumin (BSA)/phosphate buffered saline (PBS) for blocking nonspecific reactions. They were next incubated overnight at 4 °C with the goat antibody against IDS (10 μg/ml) in 1% BSA/PBS, followed by biotinylated rabbit anti-goat IgG (1:100, Vector Laboratories Inc.) for 2 h at room temperature. The reaction products were visualized by using a *Vecstain* ABC Peroxidase Kit (Vector Laboratories Inc.) and diaminobenzidine, and counterstained with Mayer's hematoxylin. They were observed under the Microscope BX40.

For the double immunofluorescence study, after the endogenous peroxidase activity had been quenched, brain sections were incubated for 20 min in 0.1% Sudan black B/70% ethanol for blocking autofluorescence. After pretreatment with *TNB* blocking buffer (PerkinElmer Inc., Waltham, MA, USA), they were incubated overnight at 4 °C with the goat antibody against IDS (2 μg/ml) and primary antibody against Lamp2 (1:500; made in mouse, Developmental Studies Hybridoma Bank at the Univ. of Iowa, Iowa, IA, USA), NSE (1:50; made in rabbit, AB951, Chemicon International Inc., Temecula, CA, USA), transferrin (1:50; made in rabbit, A0061, Dako A/S, Glostrup, Denmark), S-100 (1:50; made in rabbit, Z0311, Dako A/S) or CD68 (1:50; made in mouse, M0876, Dako A/S) in 1% BSA/PBS, followed by the peroxidase-labeled horse anti-goat IgG (1:100) and biotinylated horse anti-mouse/rabbit IgG (1:100, Vector Laboratories Inc.) for 2 h at room temperature. They were subsequently incubated in *TSA Plus* fluorescence reagent working solution (1:50, PerkinElmer Inc.) for 5 min, followed by *Texas Red* streptavidin (1:100, Vector Laboratories Inc.) for 2 h at room temperature, and mounted by using *Vectashield* mounting medium with DAPI (Vector Laboratories Inc.). Fluorescence was observed under a laser scanning confocal microscope LSM 510 META (Carl Zeiss MicroImaging GmbH, Jena, Germany).

Frozen liver sections were fixed by immersion in 4% paraformaldehyde solution for 10 min at room temperature. After quenching endogenous peroxidase activity, they were incubated for 30 min in 0.1% Triton X-100/the *TNB* blocking buffer with Avidin D solution (in Avidin/Biotin Blocking Kit, Vector Laboratories Inc.). They were next incubated overnight at 4 °C with the goat antibody against IDS (2 μg/ml) in 1% BSA/PBS with Biotin solution (in the Avidin/Biotin Blocking Kit) and subsequently with the peroxidase-labeled horse anti-goat IgG (1:100) for 30 min at room temperature. As a negative control, the sections reacted with IDS antibody which had been preabsorbed overnight at 4 °C with an excess amount (20 μg/ml) of the recombinant human IDS. They were subsequently incubated in Biotinyl *TSA* reagent working solution (1:50, PerkinElmer Inc.) for 10 min, followed by Streptavidin horseradish peroxidase (1:100, provided in the *TSA* kit) for 30 min at room temperature. After having been visualized by use of diaminobenzidine, the reaction products were counterstained and observed as described above.

A double immunofluorescence study using the antibody against IDS (2 μg/ml) and CD68 (1:50) was also performed as described above.

3. Results

3.1. Brain MR imaging before and after CBSCT

The patient's brain MR images just before CBSCT showed evidence of brain atrophy including widening of the cortical sulci and ventricles (Fig. 1A and B). The fluid-attenuated inversion recovery image also revealed enlarged Virchow–Robin spaces (Fig. 1B, arrowheads) and an abnormally high intensity of the white matter (Fig. 1B, arrows). At 7 months post-CBSCT, calculation using the software for structural image evaluation of atrophy (*SIENA* [25]; a part of Functional MRI of the Brain Software Library, *FSL* [26]) estimated the rate of brain volume loss to be 9.9% for 7 months, indicating the progression of brain atrophy (Fig. 1C). This reduced volume may have been due to not only the procedure of HSCT [27] but also the natural course of MPS II. These findings indicate that the patient had the CNS abnormalities of MPS II before CBSCT and that the brain atrophy was progressive after CBSCT.

3.2. Detection of accumulated substrate

At autopsy, the crown-heel length was 116 cm and the body weight was 25.4 kg. The brain was 935 g in weight and showed marked dilatation of the lateral ventricles and widening of the cortical sulci. Histologically, the neurons in the cerebral cortex seemed to be reduced in number with reactive gliosis and

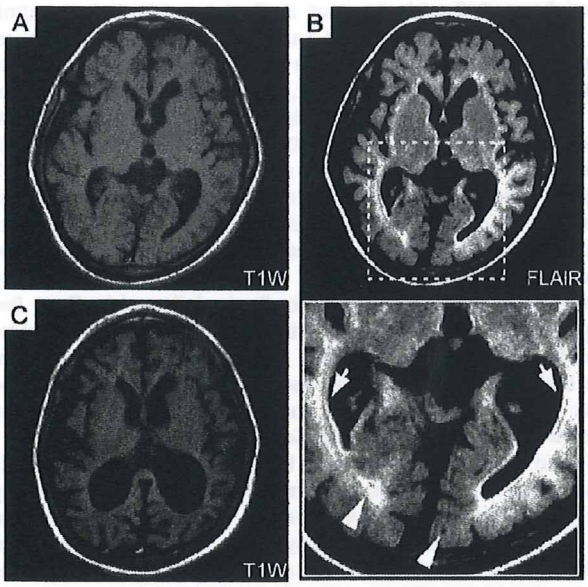

Fig. 1. MR images of our MPS II patient just before CBSCT (A and B) and at 7 months post-CBSCT (C). A and C, T1-weighted image; B, fluid-attenuated inversion recovery (FLAIR) image. The lower figure in "B" is an enlarged view of the square outlined in the upper figure in "B". Just before CBSCT, the whole brain is atrophic, and the cortical sulci and ventricles are enlarged (A and B). The enlargement of Virchow-Robin spaces (B, arrowheads) and abnormally high intensity of the white matter (B, arrows) are evident. At 7 months post-CBSCT, evidence of the progression of brain atrophy is observed (C).

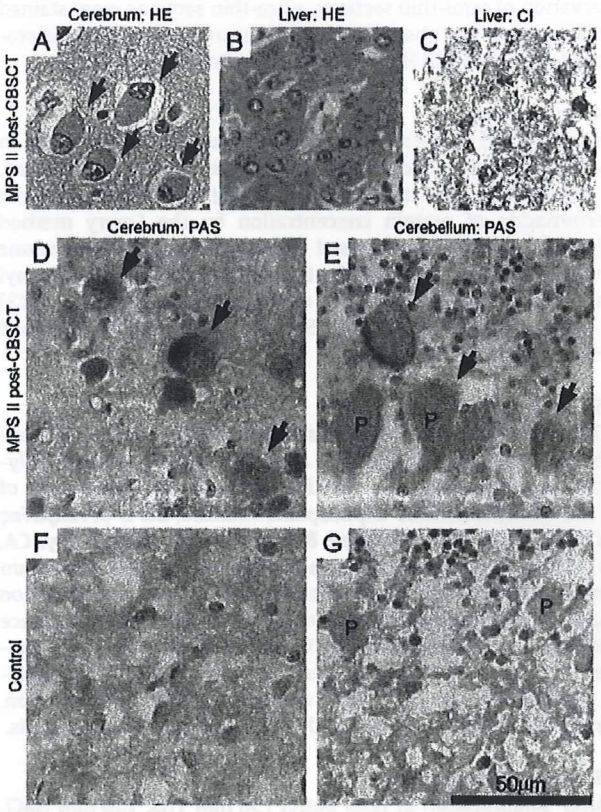

Fig. 2. (A–C) Hematoxylin and eosin (HE) staining (A and B) and colloidal iron (CI) staining (C) of MPS II post-CBSCT. A, cerebrum; B and C, liver. Neurons (A, arrows), but not hepatocytes (B), show cytoplasmic ballooning. Hepatocytes are not stainable with colloidal iron (C). D–G, PAS staining of MPS II post-CBSCT (D and E) and non-MPS II control (F and G). D and F, cerebrum and E and G, cerebellum. Many PAS-positive cells (D and E; arrows) are observed in the MPS II post-CBSCT, whereas no PAS-positive neurons are observed in the non-MPS II control. P, cerebellar Purkinje cells.

showed moderate cytoplasmic ballooning (Fig. 2A, arrows). On the other hand, the liver weight (1645 g) had increased (standard liver weight calculated with reference to the body surface area was 650 g [28]); and the edge of the organ was dull. However, hepatocytes and Kupffer cells did not appear to be swollen with vacuolar changes (Fig. 2B), and most of them were not stainable with colloidal iron (Fig. 2C). The CNS showed many PAS-positive cells in the MPS II post-CBSCT (Fig. 2D and E, arrows), whereas no PAS-positive neurons were observed in the non-MPS II control (Fig. 2F and G). Toluidine blue-stained cerebellar Purkinje cells were also ballooned (Fig. 3A, asterisks), and membranous cytoplasmic bodies were observed in these cells on electron micrographs (Fig. 3B). In addition, many phagocytic cells with enlarged intracytoplasmic vacuoles in the Virchow–Robin spaces were observed in the toluidine blue-stained sections (Fig. 3C, arrows) and on electron micrographs (Fig. 3D).

These results indicate that the characteristic abnormal findings of MPS II and the accumulated substrate had persisted in the CNS of the patient at 10 months post-CBSCT, although the characteristic pathology was not observed in the liver.

3.3. IDS enzyme activity and VNTR analysis

After confirming that the IDS enzyme activity of normal fibroblasts (88.7 nmol/4 h/mg) was in the normal range (31–110 nmol/4 h/mg [21]) by our assay, we measured IDS activity in cerebrum and liver of the normal control, the patient (MPS II post-CBSCT), and the untreated MPS II (Table 1). IDS enzyme activity in the cerebrum of the patient, as well as in that of the untreated MPS II, was only about 1% of that of the normal control. On the other hand, in the liver of the patient, it was about 40% of that of the normal control.

The analysis of the VNTR locus D1S80 revealed that the recipient blood (pre-CBSCT) showed a single band (about 600 bp; Fig. 4, black arrow) and the donor cord blood had two bands due

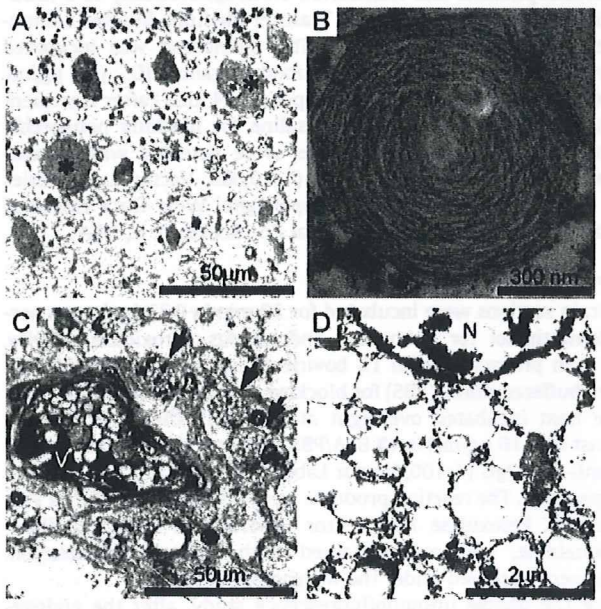

Fig. 3. Toluidine blue-stained semi-thin sections (A and C) and corresponding electron micrographs (B and D) of MPS II post-CBSCT. In the cerebellum, Purkinje cells are ballooned (A, asterisks) with membranous cytoplasmic bodies (B). In the Virchow–Robin space, many enlarged cells filled with vacuoles are observed (C, arrows; D). V, blood vessel; N, nucleus of a vacuolated cell.